Available online at www.sciencedirect.com
ScienceDirect
Geochimica et Cosmochimica Acta 74 (2010) 5494–5513
Geochimica et Cosmochimica Acta
www.elsevier.com/locate/gca

Rare earth element abundances in hydrothermal fluids from the Manus Basin, Papua New Guinea: Indicators of sub-seafloor hydrothermal processes in back-arc basins

Paul R. Craddock [a,*,1], Wolfgang Bach [b], Jeffrey S. Seewald [a], Olivier J. Rouxel [a,c], Eoghan Reeves [a], Margaret K. Tivey [a]

[a] Department of Marine Chemistry and Geochemistry, Woods Hole Oceanographic Institution, 360 Woods Hole Road, Woods Hole, MA 02543, USA
[b] University of Bremen, Geosciences Department, Klagenfurter Straße, 28359 Bremen, Germany
[c] Université Européene de Bretagne, Institut Universitaire Européen de la Mer, 29280 Plouzané, France

Received 6 July 2009; accepted in revised form 14 June 2010; available online 14 July 2010

Abstract

Rare earth element (REE) concentrations are reported for a large suite of seafloor vent fluids from four hydrothermal systems in the Manus back-arc basin (Vienna Woods, PACMANUS, DESMOS and SuSu Knolls vent areas). Sampled vent fluids show a wide range of absolute REE concentrations and chondrite-normalized (REE_N) distribution patterns ($La_N/Sm_N \sim 0.6–11$; $La_N/Yb_N \sim 0.6–71$; $Eu_N/Eu_N^* \sim 1–55$). REE_N distribution patterns in different vent fluids range from light-REE enriched, to mid- and heavy-REE enriched, to flat, and have a range of positive Eu-anomalies. This heterogeneity contrasts markedly with relatively uniform REE_N distribution patterns of mid-ocean ridge hydrothermal fluids. In Manus Basin fluids, aqueous REE compositions do not inherit directly or show a clear relationship with the REE compositions of primary crustal rocks with which hydrothermal fluids interact. These results suggest that the REEs are less sensitive indicators of primary crustal rock composition despite crustal rocks being the dominant source of REEs in submarine hydrothermal fluids. In contrast, differences in aqueous REE compositions are consistently correlated with differences in fluid pH and ligand (chloride, fluoride and sulfate) concentrations. Our results suggest that the REEs can be used as an indicator of the type of magmatic acid volatile (i.e., presence of HF, SO_2) degassing in submarine hydrothermal systems. Additional fluid data suggest that near-seafloor mixing between high-temperature hydrothermal fluid and locally entrained seawater at many vent areas in the Manus Basin causes anhydrite precipitation. Anhydrite effectively incorporates REE and likely affects measured fluid REE concentrations, but does not affect their relative distributions.

1. INTRODUCTION

Rare earth element (REE) distributions in submarine hydrothermal fluids have been used extensively as a tracer of sub-seafloor processes associated with hydrothermal activity including crustal (i.e., aluminosilicate) alteration by high-temperature hydrothermal fluids. Studies of REEs in seafloor vent fluids have focused mostly on basalt-hosted hydrothermal systems along mid-ocean ridge (MOR) spreading centers where fluids have remarkably uniform chondrite-normalized REE (REE_N) distribution patterns characterized by a light-REE enrichment and large, positive Eu anomaly (Michard et al., 1983; Michard and Albarede, 1986; Michard, 1989; Klinkhammer et al., 1994; Mitra et al., 1994; Bau and Dulski, 1999; Douville et al., 1999). REE enrichments in seafloor hydrothermal fluids relative

* Corresponding author. Tel.: +1 773 834 3997.
E-mail address: craddock@uchicago.edu (P.R. Craddock).
[1] Present address: Origins Laboratory, Department of Geophysical Sciences, University of Chicago, 5734 South Ellis Avenue, Chicago, IL 60637, USA.

0016-7037/$ - see front matter © 2010 Elsevier Ltd. All rights reserved.
doi:10.1016/j.gca.2010.07.003

to ambient seawater reflect removal from crustal rock during fluid–rock reaction. It has been suggested that plagioclase dissolution controls the distribution of REEs in submarine hydrothermal fluids because the chondrite-normalized REE (REE_N) compositions of MOR hydrothermal fluids and plagioclase are similar (Campbell et al., 1988; Klinkhammer et al., 1994). Laboratory studies, however, suggest that REE compositions of seafloor vent fluids are unrelated to primary rock composition because REE_N distribution patterns in experimental hydrothermal solutions are different from primary REE_N compositions of the volcanic rock or individual minerals with which these fluids have reacted (Bach and Irber, 1998; Möller, 2002; Allen and Seyfried, 2005). These studies suggest that vent fluid REE compositions reflect solubility control during fluid–rock interaction influenced by aqueous REE speciation (c.f., Bau, 1991), which in turn is strongly influenced by numerous aspects of fluid chemistry such as pH, temperature and the availability of ligands. Collectively, these factors lead to fractionation of REEs in sub-seafloor environments.

This study reports REE data for 36 seafloor vent fluids from four active hydrothermal systems (Vienna Woods, PACMANUS, DESMOS and SuSu Knolls) in the Manus back-arc basin, Papua New Guinea. Prior to this study, limited data existed for REE compositions of vent fluids and deposits (e.g., anhydrite) recovered from the Manus Basin or other back-arc basins (e.g., Douville et al., 1999; Bach et al., 2003). Bach et al. (2003) proposed that the heterogeneous REE_N patterns recorded by anhydrite recovered from PACMANUS reflected differences in aqueous REE concentrations that are associated with changes in fluid composition (Cl^-, F^- and SO_4^{2-} ligand concentrations) owing to varying inputs of magmatic volatiles (H_2O–CO_2–SO_2–HCl–HF). The Manus Basin is an ideal area to investigate factors that govern the aqueous abundance of REEs because the composition of underlying crustal rocks differs significantly among vent fields, ranging from basalt to rhyolite (Sinton et al., 2003; Bach et al., 2007; Sun et al., 2007). In addition, vent fluid composition (e.g., pH and ligand concentrations) and temperature differ substantially between fields owing to varying degrees of magmatic volatile degassing either on-going or in the recent past (Seewald et al., 2006; Reeves, 2010). Our data are used to examine the relationship between measured aqueous REE concentrations and host rock compositions to assess whether aqueous REE abundances are controlled primarily by crustal rock composition or aspects of fluid chemistry that affect REE solubility during sub-seafloor fluid–rock interaction. Following on from the study of Bach et al. (2003), our data are also used to examine the sensitivity of aqueous REE abundances to different fluid compositions owing to varying styles of magmatic acid volatile input. The present study provides a better understanding of how measured REE abundances in seafloor vent fluids can be used as tracers of sub-seafloor processes affecting the formation of submarine hydrothermal fluids.

2. GEOLOGIC SETTING

The Manus Basin in the Bismarck Sea, Papua New Guinea (Fig. 1) is a rapidly-opening (~100 mm/year) back-arc basin associated with subduction of the Solomon Microplate beneath the New Britain arc (Taylor, 1979; Davies et al., 1987; Martinez and Taylor, 1996). Crustal extension and spreading are complex and variable and occur along several distinct lineations. Toward the west is the Manus Spreading Center (MSC) bounded between the Willaumez and Djaul transform faults (Martinez and Taylor, 1996). Lavas erupted at the MSC are dominantly basaltic in composition (Both et al., 1986; Sinton et al., 2003; Bach et al., 2007). Several areas of hydrothermal activity have been identified in the MSC; Vienna Woods is the largest and most active of the known fields (Tufar, 1990; Tivey et al., 2007). It is located slightly south of the major spreading center within an axial rift valley at a water depth of ~2500 m.

To the east, the Eastern Manus Basin (EMB) is bounded by the Djaul and Weitin transform faults where rapid spreading is accommodated primarily by rifting and extension of existing crust (Martinez and Taylor, 1996). Lavas are erupted as a series of discrete *en echelon* neovolcanic ridges and volcanic cones of felsic (andesite to rhyolite) composition (Sinton et al., 2003; Bach et al., 2007). The arc-affinity of volcanic lavas (Sinton et al., 2003) is consistent with the proximal location (<200 km) of the EMB to the actively subducting margin. The EMB hosts several known active hydrothermal systems. The Papua New Guinea–Australia–Canada–Manus (PACMANUS) hydrothermal system is located on the crest of the 35 km long, 500 m high Pual Ridge, between water depths of 1650 and 1740 m (Binns and Scott, 1993). The ridge is constructed of several sub-horizontal lava flows with compositions between andesite and dacite (Binns and Scott, 1993; Sinton et al., 2003). There are several discrete vent fields within the PACMANUS system (Fig. 1B) that exhibit varying styles of hydrothermal activity ranging from high-temperature (>300 °C) black smoker fluid venting from sulfide-rich chimneys to low-temperature diffuse flows through sediment and cracks in lavas. Further to the east, the DESMOS and SuSu Knolls hydrothermal systems are located on individual volcanic structures in environments that are markedly different from the ridge-hosted Vienna Woods and PACMANUS hydrothermal fields. DESMOS (Onsen Field, Sakai et al., 1991; Gamo et al., 1997) is located at the crescent-shaped North wall of a caldera located in a water depth of ~1900–2000 m. Basaltic to andesitic pillow flows and hyaloclastite deposits arranged across several terraces form the slopes of the caldera. Sedimentation and alteration of primary lavas is common and includes Fe-oxide staining and acid-sulfate (advanced-argillic) alteration, locally abundant native sulfur flows and extensive presumed microbial mats (Sakai et al., 1991; Gamo et al., 1997; Gena et al., 2001). Further east, SuSu Knolls consists of three discrete volcanic cones (Suzette, North Su and South Su; Fig. 1C) at water depths between ~1140 and 1510 m (Binns et al., 1997; Tivey et al., 2007). The North Su and South Su volcanic structures are composed of abundant porphyritic dacite flows showing variable acid-sulfate type alteration (i.e., quartz–pyrophyllite–illite–alunite and native sulfur) and sedimentation by mixed volcaniclastic and hydrothermal material (Binns et al., 1997; Yeats

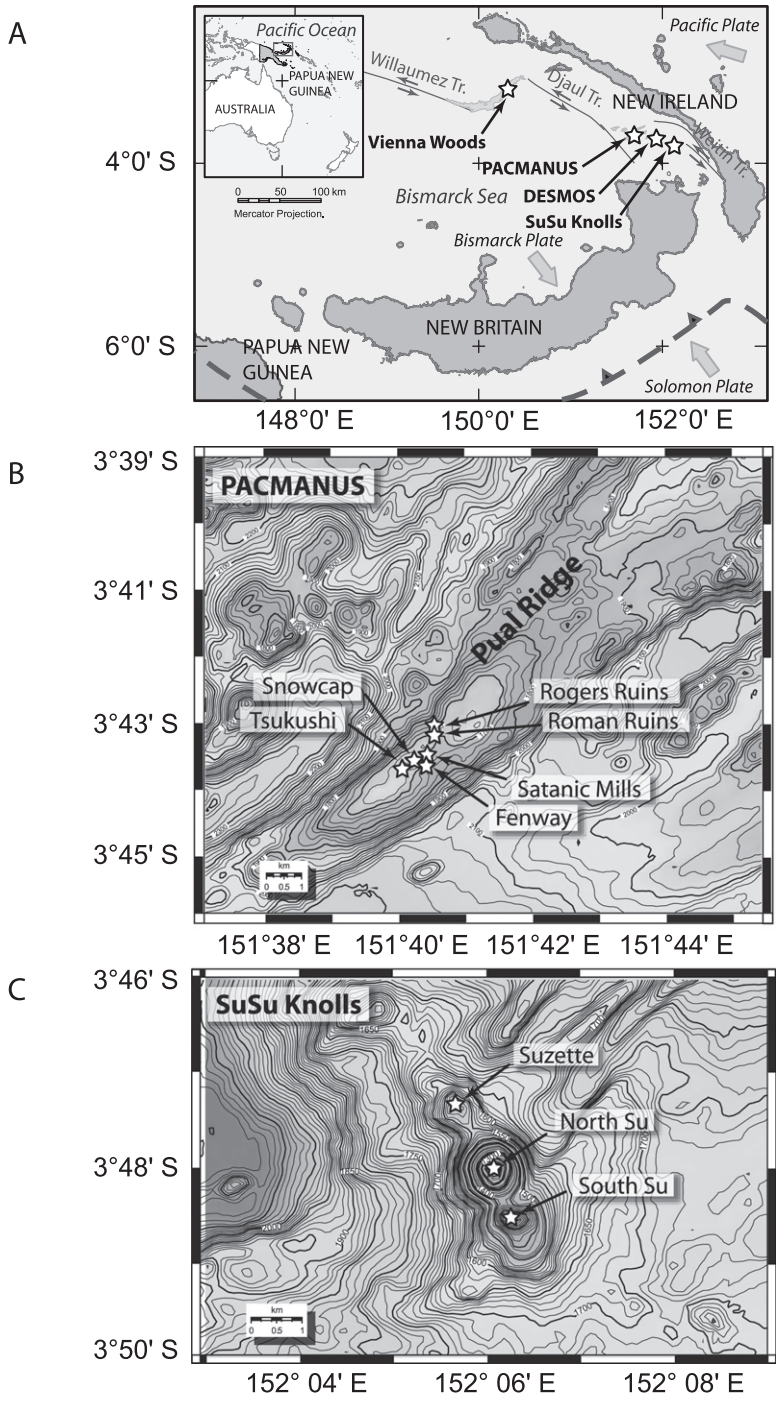

Fig. 1. (A) Regional tectonic setting of the Manus back-arc basin showing major plates and active plate motions (solid gray arrows). Areas of known hydrothermal activity in the Manus Spreading Center (Vienna Woods) and Eastern Manus Basin (PACMANUS, DESMOS and SuSu Knolls) are indicated by white stars. (B) Spatial distribution of known vent deposits at PACMANUS. (C) Spatial distribution of known hydrothermal deposits at SuSu Knolls. Seafloor bathymetry based on EM300 SeaBeam sonar (modified from Tivey et al., 2007).

et al., 2000; Hrischeva et al., 2007; Tivey et al., 2007). The Suzette volcanic structure is extensively coated in metalliferous sediment and relict sulfide talus that overlies primary and/or secondary volcanic features (Hrischeva et al., 2007; Tivey et al., 2007).

2.1. Hydrothermal activity

2.1.1. Vienna woods

Current hydrothermal activity is manifest as both focused and diffuse fluid venting within an area of ~150 m

by 100 m (Tufar, 1990; Tivey et al., 2007). Inactive sulfide chimneys extend across a total area ~300 m by 100 m. Mildly acidic (pH (25 °C) 4.2–4.7), clear and gray-smoker fluids with temperatures between 273 and 283 °C were sampled exiting the tops of large sulfide-rich chimneys up to 7 m in height (Seewald et al., 2006).

2.1.2. PACMANUS

Current hydrothermal activity occurs at several discrete vent fields (Roman Ruins, Roger's Ruins, Satanic Mills, Snowcap, Tsukushi and Fenway) that are each between 50 and 200 m in diameter (Binns et al., 2007; Tivey et al., 2007). Vent fluids with a range of temperature and composition were sampled from these fields, including high-temperature fluids (~300–358 °C) with focused discharge from black smoker chimneys, lower temperature white/gray-smoker fluids (150–290 °C) discharging from "diffuser" chimneys that lack a central open conduit, and low-temperature diffuse fluids (<100 °C) exiting through cracks in the volcanic basement or metalliferous deposits and sediments. The measured pH (25 °C) of all high-temperature vent fluids (>240 °C) are relatively acidic between 2.3 and 2.8 (Seewald et al., 2006).

2.1.3. DESMOS

Hydrothermal activity occurs at the Onsen field (Gamo et al., 1997), which is a small (~30 m diameter) area of moderate temperature fluid discharge located along the northern interior slope of the DESMOS caldera. Seafloor venting is markedly different from high-temperature black smoker fluids and is manifest as thick, milky-white fluids discharging directly through extensively altered volcanic breccia and hydrothermal sediments composed of abundant native sulfur and anhydrite (Gamo et al., 1997; Seewald et al., 2006; Bach et al., 2007). Despite the low-temperatures of sampled fluids (<120 °C), measured pH (25 °C) values are low (<1.5) and aqueous sulfate abundances exceed that of seawater concentrations (Seewald et al., 2006). On the basis of aqueous compositions, these fluids have been termed 'acid-sulfate' fluids (Gamo et al., 1997).

2.1.4. SuSu Knolls

At SuSu Knolls, hydrothermal activity and vent fluid compositions are remarkably diverse (Seewald et al., 2006). At North Su, the summit of the volcano is dominated by a large sulfide-rich black smoker complex with individual chimneys up to 11 m in height. Vent fluids sampled from this complex are similar to high-temperature black smoker fluids sampled from PACMANUS, with temperatures between 300 and 325 °C and moderate-to-low pH (25 °C) between 2.8 and 3.2 (Seewald et al., 2006). In contrast, the flanks of the volcano are dominated by extensive discharge of acid-sulfate fluids similar to that sampled from DESMOS. acid-sulfate fluids from North Su have a milky-white color, lower temperatures (48 to 241 °C), are very acidic (pH (25 °C)<1.8) (Seewald et al., 2006) and exit through cracks in hyaloclastite flows, extensively altered volcanic breccia and hydrothermal sediments composed of native sulfur and anhydrite (Yeats et al., 2000; Bach et al., 2007; Tivey et al., 2007).

There is currently more limited hydrothermal activity at South Su. This vent field is characterized by outcrops of both fresh and variably altered volcanics overlain by mostly inactive sulfide chimneys and scattered oxide-stained hydrothermal sediments (Yeats et al., 2000; Hrischeva et al., 2007; Tivey et al., 2007). In an area of diffuse venting toward the NW, extensively altered and bleached volcanic rocks were observed (Tivey et al., 2007). High-temperature fluid venting from scattered diffuser-type chimneys was observed and sampled in two areas toward the S and SE. The maximum measured temperature for these fluids was 290 °C. The pH (25 °C) of these fluids is low, ranging from 2.6 to 2.7 (Seewald et al., 2006).

The smaller structure of Suzette, located NW of North Su and South Su, is extensively covered by volcanic breccia, hydrothermal and hemipelagic sediment, mass-wasted sulfide talus, Fe-oxide crusts and limited exposures of possible hydrothermal stockwork (Hrischeva et al., 2007; Tivey et al., 2007). The summit is characterized by large expanses of both relict and scattered active sulfide chimneys that are commonly buried within thick sediment. Hydrothermal activity is intermittent over broad sections of the Suzette mound. Five high-temperature vents, with fluids emanating from sulfide-rich chimney edifices, were sampled. Temperatures ranged from 226 to 303 °C and measured pH (25 °C) from 3.5 to 3.8 (Seewald et al., 2006). A sixth fluid was sampled from a cracked pavement structure; this fluid had a temperature of ~249 °C and a considerably lower pH (25 °C) of ~2.3 (Seewald et al., 2006).

3. METHODS

3.1. Sample collection and processing

A total of 101 hydrothermal fluid samples were collected from 36 vents during *R/V Melville* cruise MGLN06MV (July–September, 2006) using discrete samplers deployed by ROV *Jason II*. Samples were primarily collected in 160 ml isobaric gas-tight samplers (Seewald et al., 2002) and supplemented with fluids collected in 755 ml Ti-syringe or "major" samplers (Von Damm et al., 1985). In most cases, fluids were sampled in triplicate. Temperatures were measured with a thermocouple mounted directly on the snorkel of the isobaric samplers, and in some cases, using the ROV temperature probe. Estimated uncertainty in the measured temperatures is ±2 °C.

Sample aliquots for chemical analysis were extracted immediately after recovery of the samplers at the end of each dive operation. Fluid samples were drawn into acid cleaned, high-density polyethylene (HDPE) Nalgene™ bottles. Aliquots of fluid drawn for REE and other trace element analysis were immediately acidified to pH < 2 by addition of Fisher Optima™ grade HCl to prevent precipitation of metal sulfides and sulfates from solution during storage prior to on-shore analysis. In nearly all major and gas-tight samplers, a precipitate ("dregs" fraction) formed on the interior walls and bottom of the sampler as the hydrothermal fluid cooled. The dregs were collected on a 0.22 μm pore-size, 45 mm diameter Nylon filter by rinsing with high-purity acetone and Milli-Q water. The

Nylon filters were dried and stored in glass vials for onshore processing. In addition, minor precipitates formed within several acidified aliquots during storage (referred to here as "bottle-filter" fraction). These precipitates were separated from the fluid by filtering through a 0.22 μm Nuclepore® filter as part of shore-based sample processing. The concentrations of REEs in sampled fluids were determined by separate measurement of element concentrations in all dissolved, dregs and bottle-filter fractions followed by mathematical reconstitution of the original fluid. A mass balance for REEs indicates that for fluids analyzed in this study, approximately 90% of REEs were in the dissolved phase.

Dissolved fractions were prepared for analysis by gravimetric dilution of a ~0.20 g split of each solution using 5% Fisher Optima™ grade HNO_3. Sample dilution factors were adjusted as a function of the chlorinity of the fluid to obtain a uniform 6 mM Cl concentration in all samples. This equated to between 80 and 110 times dilution of the original sample. Dilution to uniform Cl minimized the effect of variable matrix (primarily from Na^+, the major cation in solution) on analyte behavior within the plasma during analysis by inductively coupled plasma–mass spectrometry (ICP–MS). Dregs and bottle–filter fractions were treated separately. Particles were removed from filters into 30 ml Savillex™ vials by rinsing with 5 ml of concentrated Fisher Optima™ HNO_3. The vials were sealed and placed on a hot plate overnight (~70 °C) to digest particles. The resulting solutions were then evaporated to dryness. The acid digestion/evaporation step was repeated a further two times to achieve complete dissolution of the sulfide–sulfate mix. The digested particles were redissolved and quantitatively diluted in 5% HNO_3 acid for analysis.

3.2. Analytical methods

3.2.1. Determination of REE concentrations

Analyses of REE concentrations were performed on a ThermoElectron *Element2* ICP–MS at the Woods Hole Oceanographic Institution. Solutions were introduced into the plasma using a Cetac Aridus® desolvating nebulizer to reduce isobaric interferences (e.g., $^{135}Ba^{16}O^+$ on $^{151}Eu^+$). Barium- and REE-oxide formation was monitored throughout the analytical session by periodic aspiration of Ba and Ce spikes. Barium-oxide formation was significantly less than 1%. Significant interference of BaO^+ on Eu^+ would bias (decrease) the natural $^{151}Eu/^{153}Eu$ ratio (~0.916). In almost all samples no bias was observed and no correction for BaO interference was required. REE-oxide formation was typically less than 1–4% of total REE concentration. Samples were spiked with 1 ppb ^{45}Sc and ^{115}In internal standards to correct for fluctuations of the plasma during the analytical session. Unknown sample concentrations were calibrated against matrix-matched, multi-REE standards prepared from Specpure plasma solution standards. Background intensities were measured periodically by aspirating 5% HNO_3 blanks. External precision, determined by triplicate analysis of randomly selected samples across multiple analytical sessions, was ~10% (1σ).

3.2.2. Calculation of vent fluid and end-member fluid compositions

Typically, seafloor vent fluid compositions are reported as endmembers assuming that the hydrothermal fluid contains no Mg owing to quantitative Mg uptake during high-temperature fluid-rock interaction (Von Damm, 1983; Von Damm et al., 1985). Nearly all sampled fluids in this study contained measurable Mg. The presence of non-zero Mg reflects either the true non-zero Mg composition of the fluid sampled at the seafloor (e.g., owing to near-seafloor mixing between seawater and hydrothermal fluid), or artifacts during sampling owing to entrainment of seawater at the sampler snorkel. The measured Mg concentration of fluids sampled in duplicate or triplicate at each discrete vent orifice was typically near identical, which is interpreted as reflecting the true Mg concentration of the fluid exiting the seafloor. Fluids sampled in this study should not be interpreted as being compromised by seawater entrainment during sampling because it is unlikely that identical amounts of seawater (as indicated by the same Mg concentration) would be entrained in two or more independently sampled fluids. REE concentrations for all vent fluids sampled at the seafloor are therefore reported at the lowest measured Mg concentration (Table 1).

REE concentrations in smoker-type fluids are also reported as endmembers (Table 2) by extrapolation of replicate vent fluid compositions to zero Mg using least-squares linear regression forced to pass through the composition of ambient seawater (Von Damm, 1983). The concept of a zero Mg end-member hydrothermal fluid is useful for understanding the processes occurring in the sub-seafloor (e.g., high-temperature fluid–rock interaction) prior to mixing between hydrothermal fluid and seawater at or close to the seafloor. Calculation of end-member concentrations also allows direct comparison of species compositions among vent fluids examined in this and other studies.

REE concentrations in acid-sulfate fluids sampled from DESMOS and SuSu Knolls (North Su) were not extrapolated to zero Mg. Our indications are that the concept of a zero Mg end-member acid-sulfate hydrothermal fluid does not necessarily apply. Acid-sulfate fluids sampled in triplicate contain similar and consistently high Mg concentrations ($\geqslant$24 mmol/kg), but have elevated temperatures and very low pH. In contrast to typical high-temperature black- and gray-smoker fluids, acid-sulfate fluids appear to absent of convecting seawater-derived hydrothermal fluids that react extensively with fresh crustal rocks and instead appear to have formed primarily by sub-seafloor mixing of a magmatic volatile phase and Mg-rich seawater (Seewald et al., 2006) followed by reaction with extensively altered crustal rocks.

4. RESULTS

4.1. Rare earth element concentrations in Manus Basin hydrothermal fluids

4.1.1. Manus Spreading Center (Vienna Woods)

Total REE concentrations (ΣREE) at Vienna Woods range from ~2.6 to 5.8 nmol/kg (Table 1). Chondrite-normalized REE_N distribution patterns are uniformly

Table 1
Rare earth element concentrations (pmol/kg) in sampled smoker- and acid-sulfate-type fluids from the Manus Basin. Data are reported at the lowest measured Mg.

Sample	Vent Site	Temp (°C)	pH (25 °C)	Mg (mM)	La	Ce	Pr	Nd	Sm	Eu	Gd	Tb	Dy	Ho	Er	Yb	ΣF/ΣCl (×1000)	$\Sigma SO_4/\Sigma Cl$ (×1000)	ΣCa/ΣCl
Smoker fluids																			
VW1	Vienna Woods	282	4.4	1.4	1700	1750	180	532	88	738	81	14	43	14	30	21	0.03	0.9	0.116
VW2	Vienna Woods	273	4.2	1.0	1021	1244	157	467	81	629	61	10	33	14	25	19	0.03	0.6	0.117
VW3	Vienna Woods	285	4.7	1.1	740	958	110	291	45	390	32	7	20	19	19	11	0.03	1.5	0.105
RMR1	Roman Ruins	314	2.3	7.3	8493	10,417	837	2225	520	6848	187	27	132	21	57	65	0.19	1.6	0.030
RMR2	Roman Ruins	272	2.3	15.9	979	2210	283	1134	278	2865	188	27	207	22	59	59	0.17	5.5	0.019
RMR3	Roman Ruins	278	2.5	6.4	9585	15,412	1935	7369	1568	16,075	1121	134	626	86	221	170	0.22	2.5	0.034
RMR4	Roman Ruins	341	2.6	3.6	12,500	22,500	2830	10,213	2075	11,182	1324	154	685	97	228	191	0.19	1.7	0.034
RGR1	Roger's Ruins	320	2.7	4.2	6500	11,332	1416	5926	1389	7698	959	102	438	55	135	85	0.23	2.7	0.040
RGR2	Roger's Ruins	274	2.6	8.6	1165	2225	230	868	250	1712	232	28	135	18	42	45	0.21	3.0	0.035
SM1	Satanic Mills	295	2.6	8.2	1361	3326	480	2179	685	3417	545	73	357	59	143	120	0.29	3.7	0.022
SM2	Satanic Mills	241	2.4	16.9	330	800	125	694	389	677	1583	395	2777	479	1307	965	0.63	15.6	0.013
SM3	Satanic Mills	288	2.5	9.7	1078	2481	410	2137	1050	2477	1705	258	1362	221	593	443	0.40	5.3	0.026
SC1	Snowcap	152	4.6	30.8	221	411	46	176	83	105	58	16	112	26	83	70	0.26	22.8	0.013
SC2	Snowcap	180	3.4	24.2	352	827	70	284	56	140	50	12	70	16	40	40	0.32	10.3	0.013
TK1	Tsukushi	62	5.7	44.4	309	661	73	293	80	185	70	17	95	28	75	55	0.13	38.5	0.022
F1	Fenway	329	2.5	5.8	859	1971	232	1252	1868	7362	2073	283	1338	203	530	401	0.61	4.3	0.031
F2	Fenway	343	2.7	4.7	19,716	33,980	3982	14,465	2851	8514	1979	250	1210	165	405	314	0.25	2.5	0.038
F3	Fenway	358	2.7	4.5	15,000	27,172	3400	14,000	3400	7750	2750	320	1500	205	470	290	0.29	3.9	0.039
F4	Fenway	284	2.4	8.9	3000	9130	1200	5260	1610	5060	1970	430	3100	385	1150	900	0.30	5.9	0.034
F5	Fenway	78	5.0	44.7	1960	4700	560	2070	520	1075	655	110	760	nd	210	100	0.16	52.6	0.026
SZ1	Suzette	303	3.8	4.4	3478	5736	726	2607	444	2741	291	32	163	25	65	61	0.10	2.3	0.051
SZ2	Suzette	274	3.6	8.6	3095	5250	624	2450	546	2701	373	41	192	27	76	66	0.12	2.9	0.066
SZ3	Suzette	290	3.5	5.5	3035	6237	950	4652	1300	4798	841	88	347	49	110	83	0.12	1.5	0.066
SZ4	Suzette	229	3.6	8.3	868	1767	256	1150	279	1607	214	31	125	42	53	41	0.10	2.4	0.059
SZ5	Suzette	249	2.3	6.4	2400	4094	668	3979	2561	1304	4005	739	4637	864	2486	2076	0.79	6.7	0.040
SZ6	Suzette	226	3.7	8.0	2322	4120	594	2549	606	5024	459	45	192	26	60	54	0.12	1.9	0.066
NS3	North Su	300	3.4	1.6	10,689	18,408	2075	6913	840	3089	424	41	179	29	66	60	0.21	1.1	0.046
NS5	North Su	299	3.2	7.4	836	1700	330	2031	752	2341	265	20	90	16	37	51	0.31	4.2	0.034
NS6	North Su	325	2.8	1.6	590	690	99	470	282	1502	399	59	318	54	142	147	0.48	1.4	0.052
SS1	South Su	271	2.6	5.3	536	1250	126	452	201	181	212	57	521	91	235	164	0.56	3.3	0.045
SS2	South Su	288	2.7	6.8	480	681	70	207	61	621	51	13	62	16	47	58	0.43	3.2	0.042
Acid-sulfate fluids																			
D1	DESMOS	117	1.0	46.0	17,862	54,166	7331	31,845	7830	2948	7283	1160	6980	1330	4044	3826	0.28	297.5	0.019
D2	DESMOS	70	1.4	50.4	20,805	71,826	11,431	55,550	15,736	6526	14,321	2267	13,865	2595	7773	7336	0.01	123.7	0.024
NS1	North Su	48	1.8	49.0	10,923	35,507	4755	19,616	4699	1782	4452	718	4452	876	2793	2846	0.09	78.5	0.018
NS2	North Su	215	0.9	38.8	25,597	98,058	16,244	83,537	25,511	8865	26,764	4323	26,644	5155	15,724	15,225	0.23	335.5	0.020
NS4	North Su	241	1.5	23.5	12,657	47,812	6540	29,310	9834	3549	13,534	2355	15,301	3064	9287	8503	0.94	48.0	0.012

Table 2
End-member (zero Mg) rare earth element concentrations (pmol/kg) in smoker fluids sampled in the Manus Basin.

Sample	Vent Site	Temp (°C)	pH (25 °C)	La	Ce	Pr	Nd	Sm	Eu	Gd	Tb	Dy	Ho	Er	Yb
VW1	Vienna Woods	282	4.4	1700	1750	180	532	88	738	81	14	43	14	30	21
VW2	Vienna Woods	273	4.2	1021	1244	157	467	81	629	61	10	33	14	25	19
VW3	Vienna Woods	285	4.7	740	958	110	291	45	390	32	7	20	19	19	11
RMR1	Roman Ruins	314	2.3	9918	12,164	977	2599	607	7996	219	31	154	24	67	76
RMR2	Roman Ruins	272	2.3	1392	3140	402	1612	395	4072	268	39	294	32	83	84
RMR3	Roman Ruins	278	2.5	10,829	17,413	2186	8326	1772	18,162	1267	151	708	98	249	192
RMR4	Roman Ruins	341	2.6	13,262	23,871	3002	10,835	2201	11,863	1405	164	727	103	242	202
RGR1	Roger's Ruins	320	2.7	7071	12,328	1540	6447	1511	8374	1044	111	476	60	147	92
RGR2	Roger's Ruins	274	2.6	1390	2653	274	1035	299	2042	277	34	161	21	51	53
SM1	Satanic Mills	295	2.6	1617	3950	570	2588	813	4058	647	87	424	69	170	143
SM2	Satanic Mills	241	2.4	480	1163	182	1009	566	984	2303	575	4039	697	1901	1404
SM3	Satanic Mills	288	2.5	1317	3031	501	2612	1283	3027	2084	315	1664	270	725	541
SC1	Snowcap	152	4.6	499	928	103	396	186	237	130	35	251	58	188	158
SC2	Snowcap	180	3.4	619	1454	123	500	99	246	88	21	123	28	70	70
TK1	Tsukushi	62	5.7	1470	3148	349	1397	379	881	335	81	452	135	357	262
F1	Fenway	329	2.5	959	2200	259	1397	2085	8217	2313	315	1493	226	592	448
F2	Fenway	343	2.7	21,528	37,103	4348	15,794	3113	9296	2161	273	1321	180	442	343
F3	Fenway	358	2.7	16,318	29,560	3699	15,230	3699	8431	2992	348	1632	223	511	315
F4	Fenway	284	2.4	3609	10,984	1444	6328	1937	6087	2370	517	3729	463	1383	1083
F5	Fenway	78	5.0	9925	23,799	2836	10,482	2633	5443	3317	557	3848	nd	1063	506
SZ1	Suzette	303	3.8	3777	6228	788	2831	482	2976	316	35	177	27	70	67
SZ2	Suzette	274	3.6	3660	6209	738	2897	646	3194	441	48	227	32	90	78
SZ3	Suzette	290	3.5	3368	6921	1054	5162	1442	5324	933	97	386	55	122	92
SZ4	Suzette	229	3.6	1020	2077	301	1352	327	1888	251	36	147	50	63	48
SZ5	Suzette	249	2.3	2711	4625	755	4495	2893	1473	4525	834	5239	976	2808	2345
SZ6	Suzette	226	3.7	2711	4811	693	2976	708	5866	536	52	225	30	70	63
NS3	North Su	300	3.4	10,689	18,408	2075	6913	840	3089	424	41	179	29	66	60
NS5	North Su	299	3.2	964	1960	380	2342	867	2700	306	23	104	18	43	58
NS6	North Su	325	2.8	590	690	99	470	282	1502	399	59	318	54	142	147
SS1	South Su	271	2.6	592	1381	139	499	222	201	234	63	576	101	260	181
SS2	South Su	288	2.7	547	775	80	236	69	708	58	15	71	18	53	66

light-REE (La–Nd) enriched and show a large positive Eu-anomaly (Fig. 2). The data are consistent with REE compositions previously reported for Vienna Woods hydrothermal fluids (Douville et al., 1999). The range of REE concentrations and relative distributions are similar to those measured in high-temperature ($\geqslant$280 °C) vent fluids from basalt-hosted, mid-ocean ridge (MOR) hydrothermal sites (Fig. 2).

4.1.2. Eastern Manus Basin (PACMANUS, DESMOS and SuSu Knolls)

Most hydrothermal fluids sampled from the Eastern Manus Basin have high REE concentrations relative to fluids from Vienna Woods and overall exhibit a broad range of REE_N distribution patterns. Total concentrations of REEs at PACMANUS range from ~1.5 to 88 nmol/kg (Table 1). The REE_N distribution patterns of most sampled

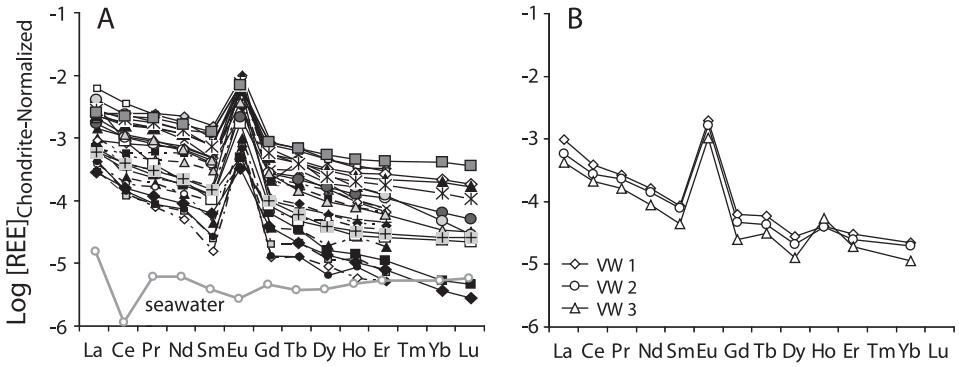

Fig. 2. Chondrite-normalized REE distribution patterns of (A) mid-ocean ridge hydrothermal fluids and modern seawater from the Pacific and Atlantic Oceans. Data are from Michard et al. (1983), Michard (1989), Klinkhammer et al. (1994), Mitra et al. (1994) and Douville et al. (1999); (B) black/gray-smoker fluids sampled from Vienna Woods, Manus Spreading Center (this study).

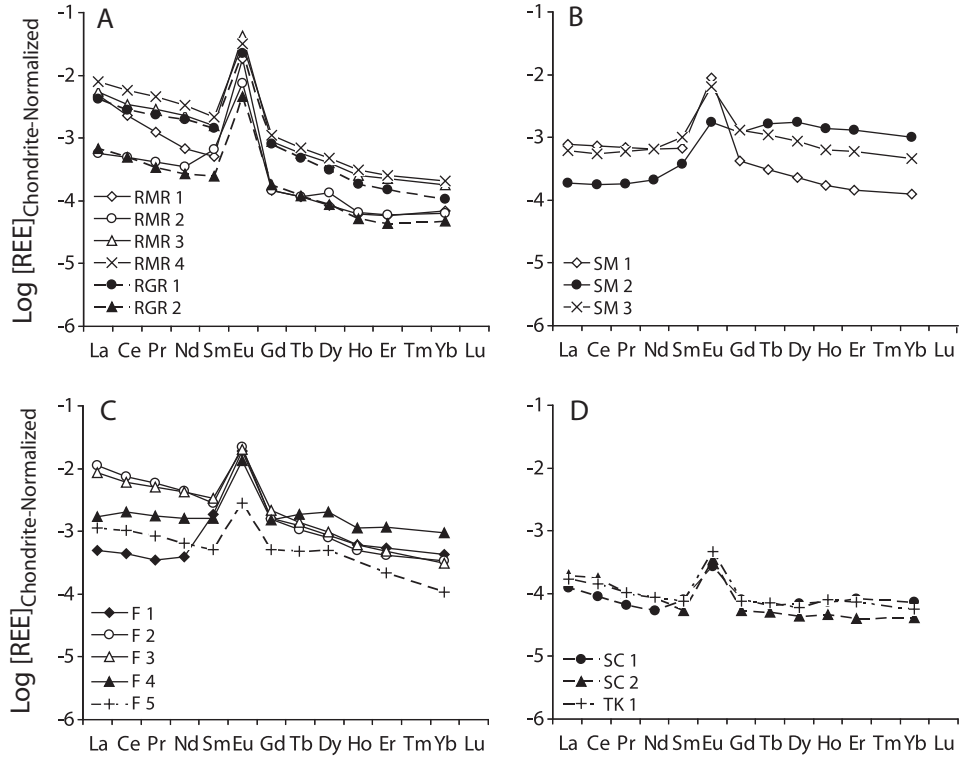

Fig. 3. Chondrite-normalized REE patterns of black/gray-smoker fluids sampled from PACMANUS, Eastern Manus Basin. (A) Roman Ruins-Roger's Ruins; (B) Satanic Mills; (C) Fenway and (D) Snowcap and Tsukushi.

fluids are variably light-REE enriched with a positive Eu anomaly (Fig. 3). Two vent fluids, Satanic Mills (vent SM2) and Fenway (vent F1), have REE_N distribution patterns that show heavy-REE (Dy–Yb) enrichments and positive Eu anomalies (Fig. 3B and C).

Total REE concentrations in acid-sulfate fluids at DESMOS vary from ~147 to 236 nmol/kg (Table 1) and are significantly greater than those of sampled high-temperature black smoker fluids at Vienna Woods and PACMANUS (see also Douville et al., 1999), but are similar to those measured in acid-sulfate fluids from continental geothermal environments (e.g., Valles Caldera, New Mexico (Michard, 1989); Rotokawa and Waiotapu, New Zealand (Wood, 2001)). Chondrite-normalized REE_N distribution patterns are generally flat with a only slight convex-upward curvature and do not have a clear positive or negative Eu anomaly (Fig. 4A). The flat REE_N distributions patterns differ markedly from those of black and gray-smoker fluids venting from chimney edifices at other vent fields.

Total REE concentrations and REE_N distribution patterns show a high degree of variability in vent fluids at SuSu Knolls (Fig. 4). Total REE concentrations in acid-sulfate fluids sampled from North Su range from ~93 to 350 nmol/kg (Table 2) and exhibit REE_N distribution patterns that are flat with no clear Eu anomaly (Fig. 4A), similar to REE_N distribution patterns in acid-sulfate fluids at DESMOS. Total concentrations of REEs in smoker fluids from North Su, South Su and Suzette range from ~6.5 to 43 nmol/kg. The REE_N distribution patterns of most black/gray-smoker fluids are light-REE enriched with pronounced positive Eu anomalies (Fig. 4B–D). Some smoker fluids sampled from Suzette (vent SZ5) and South Su (vent SS1) have REE_N distribution patterns that exhibit greater enrichment of heavy-REEs and smaller Eu anomalies relative to other smoker fluids sampled from the same vent field (Fig. 4B and D).

5. DISCUSSION

5.1. Controls on aqueous REE compositions of seafloor hydrothermal fluids

Although there is consensus that the rare earth elements (REEs) in submarine hydrothermal fluids are derived principally from the oceanic crust during high-temperature fluid–rock interaction, the primary processes that control the observed chondrite-normalized REE distribution patterns of seafloor vent fluids are poorly understood. It has been hypothesized that REE_N distribution patterns of vent fluids directly reflect the REE composition of crustal host rocks or constituent minerals, such as plagioclase, subject to alteration (Campbell et al., 1988; Klinkhammer et al., 1994). Alternatively, it has been proposed that REE_N distribution patterns of vent fluids reflect equilibrium partitioning between fluid and minerals, controlled primarily by fluid chemistry (e.g., pH, redox, availability of ligands), temperature, pressure and alteration mineralogy (Bau, 1991; Bach and Irber, 1998; Bach et al., 2003; Allen and Seyfried, 2005). Previous studies reporting REE

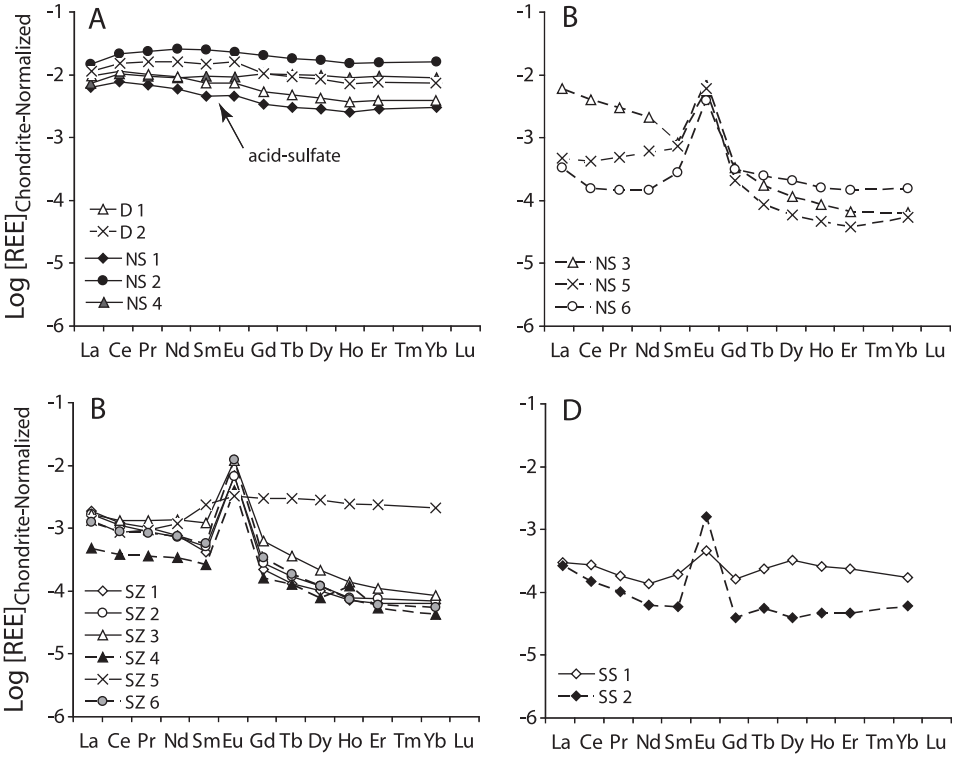

Fig. 4. Chondrite-normalized REE patterns of hydrothermal fluids sampled from DESMOS and SuSu Knolls, Eastern Manus Basin. (A) acid-sulfate fluids from DESMOS (open symbol) and North Su (filled symbol); (B) black/gray-smoker fluids from North Su; (C) black/gray-smoker fluids from Suzette and (D) black/gray-smoker fluids from South Su.

compositions of submarine hydrothermal fluids have focused largely on high-temperature, black smoker fluids sampled at mid-ocean ridge hydrothermal systems, where the range of rock-types encountered by circulating fluids is limited (i.e., all are basalt-dominated) and the compositions of sampled fluids (e.g., pH, Mg, F, SO_4^{2-} concentrations, chondrite-normalized REE patterns) are generally similar. These similar characteristics make it difficult to asses how REE solubility in submarine hydrothermal fluids is affected by changes in fluid composition and whether aqueous REE abundances reflect that of crustal rock REE compositions. In contrast, hydrothermal fluids sampled from the Manus back-arc basin have interacted with crustal rocks of a wide range of composition (from basalt to dacite and rhyolite) and are remarkably different in terms of their pH, fluid composition and ligand and REE abundances. Accordingly, these vent fluids serve as an ideal case study by which to identify the key factors that affect REE solubility at submarine hydrothermal fluids and how aqueous REE abundances can be used as tracers of hydrothermal processes.

5.1.1. *Influence of host–rock REE composition*

The range of REE_N distribution patterns observed in Manus Basin seafloor vent fluids do not reflect variations in primary whole-rock REE abundances in basalts from the Manus Spreading Center (MSC) and dacites from the Eastern Manus Basin (EMB; Fig. 5). For example, light-REE enriched patterns of Vienna Woods vent fluids are very different to whole-rock REE distribution patterns of primary basalts erupted in the MSC (Fig. 5A). Similarly, the range of REE_N distribution patterns measured in vent fluids from PACMANUS, DESMOS and SuSu Knolls is different relative to the uniform whole-rock REE distribution patterns of dacites erupted in the EMB (Fig. 5A). Moreover, the range of REE_N distribution patterns measured in Manus Basin vent fluids do not appear to record the REE composition of specific constituent minerals (see also Schnetzler and Philpotts, 1970; Hanson, 1980). In particular, the range of REE fluid compositions cannot be explained as reflecting discriminate leaching of REEs from plagioclase as previously suggested (Campbell et al., 1988; Klinkhammer et al., 1994; Douville et al., 1999). Additional evidence suggesting that vent fluid REE abundances are not controlled by primary rock composition is provided by REE concentrations and REE_N distribution patterns that vary substantially among fluids samples within individual vent areas on spatial scales (<100–500 m) over which the primary REE composition of volcanic rocks are uniform (Sinton et al., 2003; Miller et al., 2006). The fluid compositional data suggest that REEs are fractionated from primary crustal rock REE compositions during fluid–rock interaction owing to differences in aqueous REE solubility. This idea is supported by the mineral and chemical compositions of altered crustal rocks in the Manus Basin that vary significantly from chlorite–smectite (argillaceous) to illite–pyrophyllite–cristobalite–anhydrite (advanced-argillic) assemblages (Lackschewitz et al., 2004; Paulick et al., 2005; Paulick and Bach, 2006; Bach et al., 2007) and

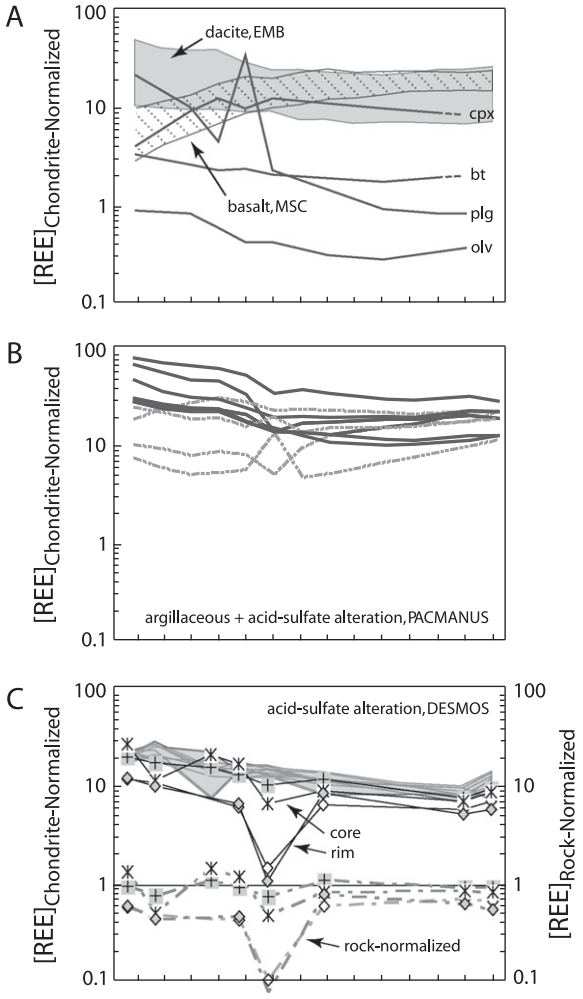

Fig. 5. REE distribution patterns of: (A) bulk primary basalts (stippled field) and bulk primary dacites (gray field) sampled along the Manus Spreading Center (MSC) and Eastern Manus Basin (EMB). Data are from Sinton et al. (2003). Also shown are characteristic REE patterns of constituent mineral phases in mafic (basalt) and felsic (dacite, rhyolite) igneous rocks (cpx is clinopyroxene, bt is biotite, plg is plagioclase and olv is olivine). Data are from Schnetzler and Philpotts (1970). Data are normalized to average chondritic composition. (B) variably altered dacites sampled from the beneath PACMANUS, in the EMB. Solid and dashed lines indicate dacites showing incipient (chlorite-smectite) and extensive ("acid-sulfate-type", illitepyrophyllite-alunite) alteration, respectively. Data are from Beaudoin et al. (2007) and are normalized to average chondritic composition. (C) bulk primary dacites (gray field) and highly-altered dacites ("acid-sulfate-type" alteration, shown in solid black lines) sampled at the DESMOS hydrothermal field, EMB. Data are normalized to average chondritic composition. Also shown are REE pattern of the highly-altered dacites normalized to that of the primary dacites (dashed gray lines). REE data are from Gena et al. (2001). The REE patterns of primary and altered rocks record evidence for significant and variable REE mobilization during fluid-rock interaction, similar to that inferred from the fluid REE compositions reported in this study. During low pH, acid-sulfate-type alteration, the REEs appear to be mobilized without significant fractionation among the lanthanides (C). See text for discussion.

indicate fluid–rock interaction involving a range of temperatures (>220–360 °C), pH (<2 to >3.5), water/rock ratios and fluid compositions. The REE compositions of variably altered rocks show a range of chondrite-normalized compositions (Fig. 5B and C) that are consistent with variable mobilization and extensive fractionation of the REEs during crustal rock alteration (e.g., Gena et al., 2001; Beaudoin et al., 2007).

5.1.2. Influence of fluid composition – pH and ligand concentration

High-temperature black smoker and acid-sulfate fluids in the Manus Basin exhibit a wide range of pH and fluid composition (e.g., alkali metal, Mg, Cl, F and SO_4 abundances) that reflect different styles of sub-seafloor fluid circulation, a range of conditions of fluid–rock interaction and variable crustal rock compositions (Seewald et al., 2006; Craddock, 2009; Reeves, 2010). The compositions of high-temperature black and gray-smoker fluids at Vienna Woods, PACMANUS and SuSu Knolls (e.g., Mg depletion and alkali metal enrichment relative to ambient seawater) reflect extensive reaction (buffering) between convecting seawater-derived hydrothermal fluids and fresh basalts in the MSC and dacites in the EMB (Craddock, 2009). The low pH and elevated F concentrations of black smoker fluids in the EMB (PACMANUS and SuSu Knolls) relative to those from the MSC (Vienna Woods) may reflect assimilation of magmatic acid volatiles (H_2O–CO_2–SO_2–HCl–HF) with convecting hydrothermal fluids owing to the proximity of EMB to the active subducting arc. Acid-sulfate fluids at DESMOS and SuSu Knolls in the EMB are products of fundamentally different styles of hydrothermal activity and are probable submarine equivalents of fumaroles associated with subaerial volcanism (Giggenbach, 1992; Hedenquist et al., 1994). These fluids appear to have formed via shallow mixing of magmatic acid volatiles with entrained seawater in the absence of large-scale seawater convective circulation and reaction with fresh crustal rocks (Seewald et al., 2006). The low pH (25 °C) < 1–1.5 and high sulfate concentrations (28–149 mmol/kg) in DESMOS and SuSu Knolls acid-sulfate fluids relative to ambient seawater (Gamo et al., 1997; Seewald et al., 2006) likely reflect addition of SO_2-rich magmatic vapors to seawater and disproportionation of SO_2 at decreasing temperatures to yield sulfuric acid (e.g., Holland, 1965). The high concentrations of Mg ($\geqslant$24 mmol/kg) and low concentrations of fluid-mobile elements (e.g., alkali metals) in acid-sulfate fluids are a critical difference relative to that of typical black smoker fluids (Craddock, 2009). These data suggest that acid-sulfate fluid compositions are not governed primarily by reaction with fresh crustal rocks, but reflect interaction with previously and variably altered crustal rocks. This idea is supported by the occurrence of highly-altered rocks containing cristobalite, alunite, pyrophyllite and native sulfur in proximity to acid-sulfate fluids at the seafloor at DESMOS and SuSu Knolls (Gamo et al., 1997; Bach et al., 2007) that are analogous to the low pH, advanced-argillic alteration observed in subaerial epithermal environments (Hemley and Jones, 1964; Hemley et al., 1969).

We propose that the range of REE abundances observed in Manus Basin hydrothermal fluids are controlled primarily by fluid composition (e.g., pH, availability of ligands) and alteration mineralogy, which regulate aqueous REE solubility during sub-seafloor fluid–rock interaction. Overall, REE concentrations in Manus Basin vent fluids increase with acidity (Fig. 6). REE concentrations in acid-sulfate fluids from DESMOS and SuSu Knolls are high relative to black and gray-smoker fluids sampled in the Manus Basin, despite the lower temperatures of acid-sulfate fluids. Similarly, REE concentrations are high in lower pH smoker fluids from PACMANUS and SuSu Knolls (pH (25 °C) 2.3–3.5) relative to higher pH smoker fluids sampled from Vienna Woods (pH (25 °C) $\geqslant$ 4.2). Similar correlations in hydrothermal fluids sampled from a range of geologic environments, including basalt-dominated mid-ocean ridge (MOR) and continental geothermal systems (Michard and Albarede, 1986; Michard, 1989; Lewis et al., 1997; Douville et al., 1999; Wood, 2001) support this relationship. It is unlikely that REE abundances in seafloor hydrothermal fluids are limited by their abundance in the host rock because the concentrations of REEs in both fresh and altered oceanic crustal rocks (e.g., Michard et al., 1983; Beaudoin et al., 2007) are several orders of magnitude higher than those measured in submarine hydrothermal fluids (see Fig. 5). Indeed, acid-sulfate fluids have the highest REE concentrations, despite these fluids having bulk aqueous compositions consistent with reaction with altered crustal rocks, which typically contain REE abundances lower than those in primary igneous lavas (e.g., Beaudoin et al., 2007). The results suggest total REE abundances in submarine hydrothermal fluids are solubility controlled during

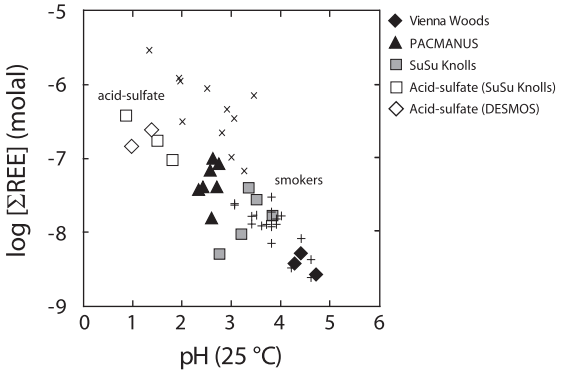

Fig. 6. Total REE abundance versus pH for black smoker and acid-sulfate fluids sampled in the Manus Basin (this study). REE concentrations in black smoker fluids from unsedimented, mid-ocean ridge hydrothermal systems (symbol +) and in acid-sulfate fluids from continental geothermal systems (symbol ×) are shown for comparison (data from Michard, 1989; Klinkhammer et al., 1994; Lewis et al., 1997; Douville et al., 1999). Smoker-type fluids with lower temperatures (<280 °C) and elevated Mg concentrations (>10 mmol/kg) are not plotted as these fluids have experienced local sub-seafloor mixing with seawater and the measured pH (25 °C) of these fluids does not reflect that of the high-temperature hydrothermal fluid at depth.

high-temperature fluid–rock interaction, are strongly influenced by pH, and are largely independent of crustal–rock REE abundances.

Sampled vent fluids are also characterized by a range of chondrite-normalized (REE_N) patterns that vary systematically with pH and the availability of aqueous ligands. These trends are readily apparent upon examination of La_N/Yb_N and Eu_N/Eu^*_N ratios as a function of relative ligand abundances (Fig. 7). The La_N/Yb_N ratio is a measure of the relative light-REE (La) versus heavy-REE (Yb) abundance and reflects chemical fractionation among the light- and heavy-REEs. The Eu_N/Eu^*_N ratio (Eu anomaly) is a measure of the fractionation of Eu relative to neighboring REEs (Sm and Gd), which can be related to the varying oxidation state exhibited by Eu (II and III) compared to trivalent REEs in high-temperature hydrothermal fluids (Sverjensky, 1984). High-temperature smoker fluids from all Manus Basin vent areas exhibit a wide range of ΣF/ΣCl ratios and a limited range of low $\Sigma SO_4/\Sigma Cl$ ratios, the latter being the result of sulfate removal by anhydrite precipitation and reduction to H_2S during fluid–rock interaction. Manus Basin smoker fluids with low F and SO_4^{2-} concentrations, and low ΣF/ΣCl (<0.03 μM/mM) and $\Sigma SO_4/\Sigma Cl$ ratios (~1 μM/mM) have a characteristic light-REE enrichment and large positive Eu-anomaly (highest La_N/Yb_N and Eu_N/Eu^*_N ratios; Fig. 7). In contrast, smoker fluids that have a range of high F concentrations and high ΣF/ΣCl ratios have only minor light-REE enrichments and lower La_N/Yb_N and Eu_N/Eu^*_N ratios. The most fluoride-rich sampled fluids with the highest ΣF/ΣCl ratios approaching ~0.60–0.80 μM/mM (Satanic Mills SM2, Fenway F1, Suzette SZ5; Table 1, Fig. 7) exhibit a distinct light-REE depletion and heavy-REE enrichment ($La_N/Yb_N \ll 1$) and a small or absent Eu anomaly ($Eu_N/Eu^*_N \sim$ 1–2).

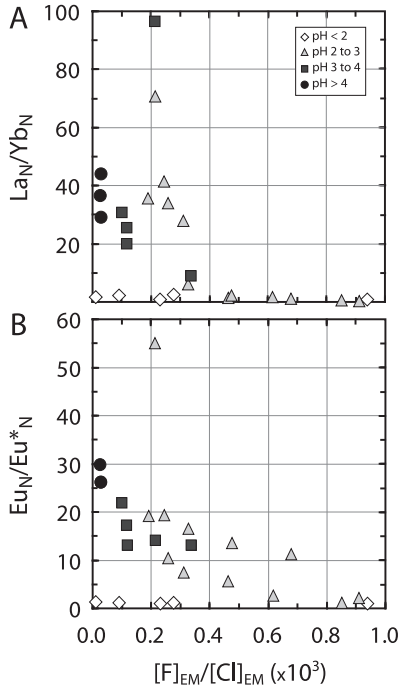

Fig. 7. Correlations between aqueous [ΣF]/[ΣCl] ratios and chondrite-normalized La_N/Yb_N (A) and Eu_N/Eu^*_N ratios (B) in black smoker and acid-sulfate fluids from the Manus Basin. Data for all vent areas are grouped by measured pH (25 °C). Smoker fluids with lower temperatures (<280 °C) and elevated Mg concentrations (>10 mmol/kg) are not plotted. Smoker fluids (pH > 2 to 4) show decreasing La_N/Yb_N and Eu_N/Eu^*_N ratios (increasing heavy-REE abundances relative to light-REEs and Eu) with increasing [ΣF]/[ΣCl] ratios. Acid-sulfate fluids (pH < 2) show no clear differences in La_N/Yb_N and Eu_N/Eu^*_N ratios for a wide range of [ΣF]/ΣCl] ratios. Differences in ligand abundances affect aqueous REE_N distributions likely owing to the formation of various REE-ligand complexes with different stabilities. See text for discussion.

We interpret the range of light- versus heavy-REE enrichments observed in these fluids as reflecting differences in relative solubilities of the light- versus heavy-REEs as a direct result of significant differences in pH, ligand concentration and, therefore, the relative abundances of REE-chloride and REE-fluoride complexes. The pronounced light-REE enrichment and positive Eu-anomaly in smoker fluids with chloride-rich, but fluoride- and sulfate-poor compositions implies that REE-chloride complexation acts to enhance the solubility of the light-REEs and Eu relative to that of the mid- and heavy-REEs during fluid–rock interaction and secondary mineral formation. In contrast, the marked heavy-REE enrichment in fluoride-rich smoker fluids suggests that formation of REE-fluoride complexes enhances the solubility of the heavy-REEs relative to light-REEs during fluid-rock interaction in the presence of elevated concentrations of fluoride.

These interpretations are supported by the results of species distribution thermodynamic calculations that were carried out to assess the aqueous speciation/complexation of REEs in representative sampled Manus hydrothermal fluids at in situ temperature and pressure across a broad range of fluid compositions (compositions of the seven fluids used for illustration in speciation calculations are given Table 3; results of calculations are presented in Fig. 8). Details of the thermodynamic calculations used in this study are documented in full in the Supporting Online Material (SOM). Briefly, calculations were carried out using the SpecE8 program, included as a module of the Geochemist's Workbench (v6.0) software package (Bethke, 1996). The SpecE8 program computes species distributions, mineral saturation states and gas fugacity in aqueous solutions at specified temperature and pressure. The thermodynamic database used in SpecE8 calculations was generated using SUPCRT 92 (Johnson et al., 1992) for a pressure of 50 MPa (500 bars) and temperatures between 0 and 400 °C, using updates for aqueous formation constants as listed in the SOM. The pH value of each fluid measured at 25 °C was used together with aqueous compositional data to calculate pH at in situ temperature. The redox potential for each fluid was calculated based on measured H_2(aq) concentrations and the assumption of H_2(aq)–H_2O equilibrium. Equilibrium between H_2S and SO_4^{2-} was suppressed because both species were measured in our hydrothermal fluids and are in a state of non-equilibrium. REE speciation in chloride-rich, but fluoride- (<20–170 μmol/kg) and sulfate-poor (<2 mmol/kg) smoker-type vent fluids

Table 3
Chemical compositions of representative hydrothermal fluids used in thermodynamic REE speciation calculations.

Sample	Vent Site	Temp (°C)	pH (25°C)	pH (in situ)	Mg (mmol/kg)	Cl (mmol/kg)	Na (mmol/kg)	K (mmol/kg)	Ca (mmol/kg)	Ba (μmol/kg)	Al (μmol/kg)	Mn (μmol/kg)	Fe (μmol/kg)	SiO_2 (mmol/kg)	SO_4 (mmol/kg)	F (μmol/kg)	CO_2 (mmol/kg)	H_2S (mmol/kg)	H_2 (μmol/kg)
Smoker Fluids																			
VW1	Vienna Woods	282	4.4	4.8	1.4	690	512	21.2	80.0	55	< 10	349	159	15.3	0.8	21	4.4	1.4	42
RMR4	Roman Ruins	341	2.6	3.37	3.6	650	495	77.2	22.3	92	< 10	2830	6468	17.8	0.4	125	9.5	6.3	53
SM1	Satanic Mills	295	2.6	3.25	8.2	519	407	60.5	12.5	20	< 10	2145	2790	12.2	2.1	167	181	8.0	25
SM2	Satanic Mills	241	2.4	3.2	16.9	455	374	38.6	5.9	16	< 10	1853	1045	12.8	7.1	287	112	4.5	4.3
SZ5	Suzette	249	2.3	2.7	6.4	610	493	44.3	24.2	16	18	243	3961	14.1	3.0	480	16.1	4.8	7.4
Acid-Sulfate Fluids																			
D1	DESMOS	117	1.0	1.2	46.0	492	391	8.3	9.4	< 1	480	40	12400	8.1	147	137	23.1	0.0	4.0
NS2	North Su	215	0.9	1.18	38.8	442	340	7.8	8.9	nd	1075	81	3103	10.0	149	128	80.0	0.0	20

is governed primarily by REE-chloride and REE-oxyhydroxide complexes of trivalent REEs and chloride complexes of divalent Eu (e.g., Vienna Woods VW1, Roman Ruins RMR4, Satanic Mills SM1; Fig. 8). REE-fluoride complexes are present in lesser amounts and REE-sulfate complexes are present at relatively low abundance. The predominance of divalent Eu versus trivalent Eu reflects the stability of Eu^{2+} under reducing conditions and elevated temperatures characteristic of sampled vent fluids (e.g., Sverjensky, 1984). The differences in the relative abundance of REE-chloride and REE-oxyhydroxide complexes result primarily from differences in fluid temperature and pH with REE-chloride complexes increasing in abundance at higher temperature and lower pH. The calculated REE speciation does not change significantly across different geologic settings and crustal compositions (e.g., basalt-dominated Vienna Woods versus dacite-dominated PACMANUS) because the fluid compositions are similar.

REE species distribution in high-temperature vent fluids with a range of elevated fluoride concentrations (up to ~500 μmol/kg) is increasingly governed by the presence of REE-fluoride complexes, which occur primarily at the expense of REE-chloride complexes (e.g., Satanic Mills SM2, Suzette SZ5, Fig. 8). The light-REEs occur predominantly as chloride complexes, but the heavy-REEs are present predominantly as fluoride complexes. The relative abundance of REE-hydroxide and REE-sulfate complexes are low; similar to that predicted for other high-temperature smoker fluids. Europium is again predicted to occur exclusively as a divalent chloride complex. Theoretical and experimental estimates of the relative stabilities of REE-chloride and REE-fluoride complexes across the lanthanide group (e.g., Wood, 1990; Haas et al., 1995; Gammons et al., 2002; Migdisov and Williams-Jones, 2007; Migdisov et al., 2009) are not without uncertainties and discrepancies (see documentation of thermodynamic data in SOM). However, these studies suggest that chloride complexes of the light-REEs and Eu^{2+} are more stable than those of the heavy-REEs at elevated temperature and pressure, whereas fluoride complexes possibly show the opposite behavior, consistent with our interpretation of natural samples. Fractionation of the REEs during fluid-rock interaction and secondary mineral formation owing to differences in complexation and solubility of the REEs is also consistent with the results of experimental studies that have demonstrated enhanced mobility of the light-REEs and divalent Eu^{2+} during fluid–rock interaction with chloride-rich hydrothermal fluids at elevated temperature and pressure (e.g., Allen and Seyfried, 2005). No experimental studies have yet investigated the relative solubility and mobility of the REEs during fluid-rock interaction in the presence of fluoride-rich hydrothermal fluids at elevated temperature and pressure.

Marked differences in fluid composition likely also govern the REE distributions observed in acid-sulfate fluids, which are distinct to those of smoker fluids. All acid-sulfate fluids exhibit almost flat REE_N distribution patterns with no Eu-anomalies ($La_N/Yb_N \sim 1$–2.5, $Eu_N/Eu^*_N \sim 1$), similar to REE_N patterns identified in other acid-sulfate fluids sampled in the Manus Basin (e.g., Douville et al., 1999).

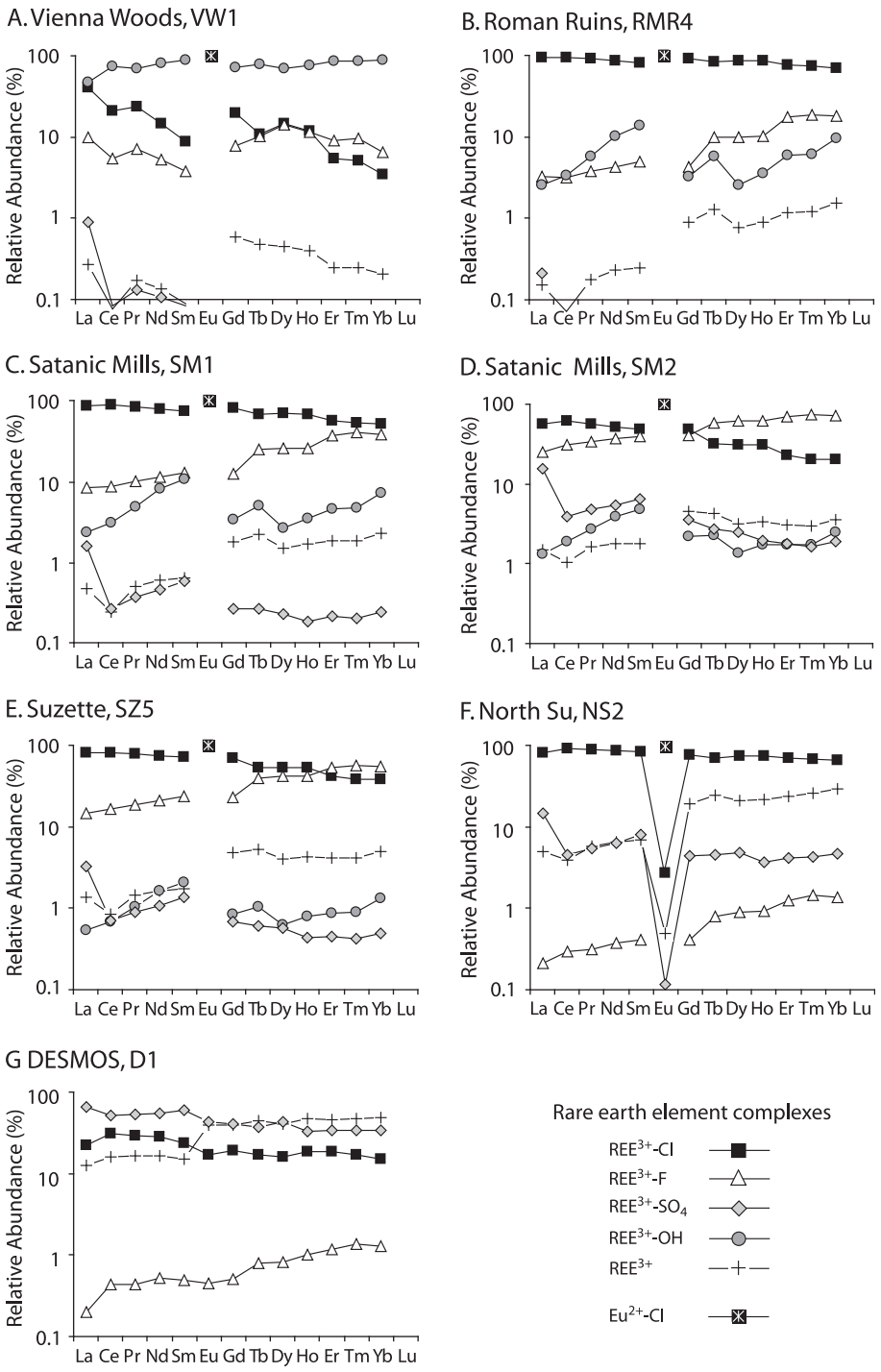

Fig. 8. Predicted REE species distributions in high-temperature smoker fluids from the Manus Basin. (A) Fluid VW1 (Vienna Woods); (B) fluid RMR4 (Roman Ruins, PACMANUS); (C) fluid SM1 (Satanic Mills, PACMANUS); (D) fluid SM2 (Satanic Mills, PACMANUS); (E) fluid SZ5 (Suzette, SuSu Knolls); (F) fluid NS2 (North Su, SuSu Knolls) and (G) fluid D1 (DESMOS). REE-chloride, REE-fluoride and REE-sulfate complexes are shown by black squares, white triangles and gray diamonds, respectively. REE-oxyhydroxide complexes are shown by gray circles and free REE ions by black crosses. Fluid compositions used in calculations are reported in Tables 1 and 3.

We interpret the high REE concentrations and flat REE_N patterns of acid-sulfate fluids as reflecting primarily the influence of low pH, which enhances the aqueous solubility of all REEs. The very low pH is likely the critical parameter controlling the observed abundances of REEs in acid-sulfate fluids because observations of natural systems suggest that the solubility of REEs during fluid-rock reaction increases significantly with acidity (Fig. 6) (e.g., Michard, 1989; Lewis et al., 1998; Fulignati et al., 1999). In effect, acid-sulfate-type alteration occurring at very low pH, as is

observed at DESMOS and SuSu Knolls, effectively leaches and mobilizes REEs from host rocks without fractionation among the lanthanides. Indeed, REE_N distribution patterns of acid-sulfate fluids are similar to that of both primary and altered felsic crustal rocks in the Eastern Manus Basin (e.g., Gena et al., 2001) with which acid-sulfate fluids have likely reacted (Fig. 5C).

Results of thermodynamic species distribution calculations suggest that formation of aqueous REE complexes in acid-sulfate fluids appears to exert a relatively minor control over the relative solubility of the REEs. REE species distribution calculations suggest that at lower temperatures relevant to most acid-sulfate fluids (<120 °C) the REEs are present in solution predominantly as free trivalent ions (e.g., DESMOS D1, Fig. 8). Similar results were obtained in REE species distribution calculations reported for acid-sulfate fluid by Douville et al. (1999) and Bach et al. (2003). Europium can occur as trivalent Eu reflecting the lower temperature and more oxidizing composition of these fluids relative to typical high-temperature smoker fluids. A low pH is critical for maintaining high concentrations of REEs in solution as uncomplexed ions. The formation of REE-sulfate complexes as predicted by species distribution calculations (owing to high sulfate concentrations in acid-sulfate fluids up to 150 mmol/kg) may further enhance REE solubility. At higher temperatures (>200 °C), thermodynamic calculations predict that REE-chloride complexes increasingly contribute to REE speciation in acid-sulfate fluids (e.g., North Su NS2; Fig. 8). Differences in the relative abundance of REE-sulfate versus REE-chloride complexes do not obviously affect overall REE abundances, suggesting that pH is the more important control. Measured REE abundances and REE_N patterns are not obviously affected by the wide range of fluoride concentrations in acid-sulfate fluids (Fig. 7), suggesting that REE-fluoride complexes do not contribute to aqueous REE speciation in these fluids. The lack of REE-fluoride complexation in acid-sulfate fluids (Figs. 8 and 9) likely reflects quantitative sequestration of fluoride as HF° at very low pH owing to the weak acid behavior of hydrofluoric acid at elevated temperature (pKa ~3.1 at 25 °C and 4.6 at 200 °C). It has also been suggested that competitive formation of Al-fluoride complexes may inhibit REE-fluoride complex formation in acid-sulfate fluids (Gimeno Serrano et al., 2000). Indeed, acid-sulfate fluids sampled in the Manus Basin have very high concentrations of dissolved Al (Table 3) and Al-fluoride complexes and HF° constitute the entirety of aqueous fluoride species in acid-sulfate fluids (Fig. 9). The presence or absence of Al-fluoride complexes, however, does not affect the predicted abundance of REE-fluoride complexes in acid-sulfate fluids because formation of Al-fluoride complexes in acid-sulfate fluids occurs predominantly at the expense of HF°, not REE-fluoride complexes (Fig. 9).

In summary, the data presented suggest that REE solubility during fluid–rock interaction at elevated temperature and pressure is critically dependent upon fluid composition – in particular pH and the concentration of aqueous REE ligands. Different REE abundances and REE_N distribution patterns among smoker- and acid-sulfate-type fluids in the

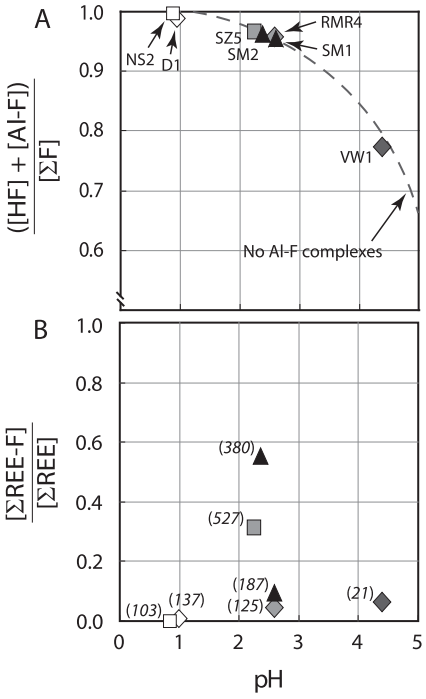

Fig. 9. Fractional abundance of (A) fluoride present in solution as HF and Al-fluoride complexes and (B) REE present in solution as REE-fluoride complexes, versus measured fluid pH (25 °C) for hydrothermal fluids listed in Table 3. The dashed line in (A) is the modeled fractional abundance of HF relative to total fluoride in the absence of Al-fluoride complexation (i.e., Al3 + removed from fluid compositions for species distribution calculations). The values in parentheses in (B) are measured fluoride concentrations. At low pH in acid-sulfate fluids, fluoride is effectively bound as HF and is unavailable to complex REEs. The presence or absence of Al-fluoride complexes does not affect predicted REE-fluoride complex abundances (dashed line follows modeled fluids). At higher pH in smoker fluids, proportionally more fluoride is dissociated and available to complex with REEs. The fraction of REE complexed with fluoride is significant in fluoride-rich (⩾400 μM) hydrothermal fluids at pH > 2.

Manus Basin likely reflect differences in REE solubility owing to variations in the relative abundance and stability of REE-chloride, fluoride and sulfate complexes as a function of different temperature, pH and ligand concentration (e.g., ΣF/ΣCl and $\Sigma SO_4/\Sigma Cl$ ratios). The observed correlations suggest that light-REE and Eu enrichments (large positive La_N/Yb_N and Eu_N/Eu_N^* ratios) are favored in hydrothermal fluids with low fluoride and sulfate concentrations (low ΣF/ΣCl and $\Sigma SO_4/\Sigma Cl$ ratios) in which REE-chloride complexes are the likely dominant REE species. In contrast, heavy-REE (and to a lesser degree mid-REE) enrichments are favored in hydrothermal fluids with high fluoride concentrations (high ΣF/ΣCl ratios) in which REE-fluoride complexes are likely important REE species. In acid-sulfate fluids, enrichment of all REEs appears to be critically dependent upon the very low pH and possibly, to a lesser extent, the presence of REE-sulfate and/or chloride complexes. Importantly, the apparent sensitivity of aqueous REE distributions to pH and Cl, F and SO_4^{2-} concentrations implies that the REEs can be used as tracers for input

of fluoride- and sulfur-rich magmatic acid volatiles (H_2O–CO_2–SO_2–HCl–HF) in seafloor hydrothermal fluids. Further, because minerals in hydrothermal vent deposits (e.g., anhydrite) often record REE distributions which preserve that of the original hydrothermal fluid, the REEs may also provide critical information about hydrothermal processes associated with the formation of seafloor vent deposits, such as fluid pH, composition and the extent and type of magmatic acid volatile input, all of which impact metal behavior and metal-sulfide mineralization.

5.1.3. Consequences of seawater entrainment and fluid mixing

Studies of MOR hydrothermal systems have demonstrated that entrainment and sub-seafloor mixing of seawater with rising high-temperature hydrothermal fluids can affect seafloor vent fluid compositions owing to mineral precipitation and/or dissolution (Edmond et al., 1995; Tivey et al., 1995). Anhydrite ($CaSO_4$) precipitation is a common product of sub-seafloor mixing between high-temperature fluids and locally entrained seawater (Tivey et al., 1995; Mills et al., 1998; Tivey et al., 1998; Mills and Tivey, 1999; Humphris and Bach, 2005) and can incorporate significant amounts of REEs (Mills and Elderfield, 1995; Humphris, 1998). Substantial amounts of anhydrite have been recovered from beneath several PACMANUS vent deposits (Binns et al., 2007; Tivey et al., 2007). The down-hole distribution of anhydrite veins in Ocean Drilling Program Leg 193 drill core from PACMANUS demonstrates widespread precipitation of anhydrite extending to depths >300 mbsf (Bach et al., 2003; Roberts et al., 2003). Sulfate–sulfur isotopic compositions of anhydrite at PACMANUS cluster around that of seawater sulfate consistent with deposition of anhydrite in response to sub-seafloor mixing between entrained seawater and high-temperature hydrothermal fluid (Roberts et al., 2003; Craddock and Bach, 2010).

The range of chemical compositions of seafloor vent fluids sampled at PACMANUS is consistent with on-going anhydrite precipitation at some vent areas (Seewald et al., 2006; Reeves, 2010). The highest-temperature ($\geqslant$340 °C)

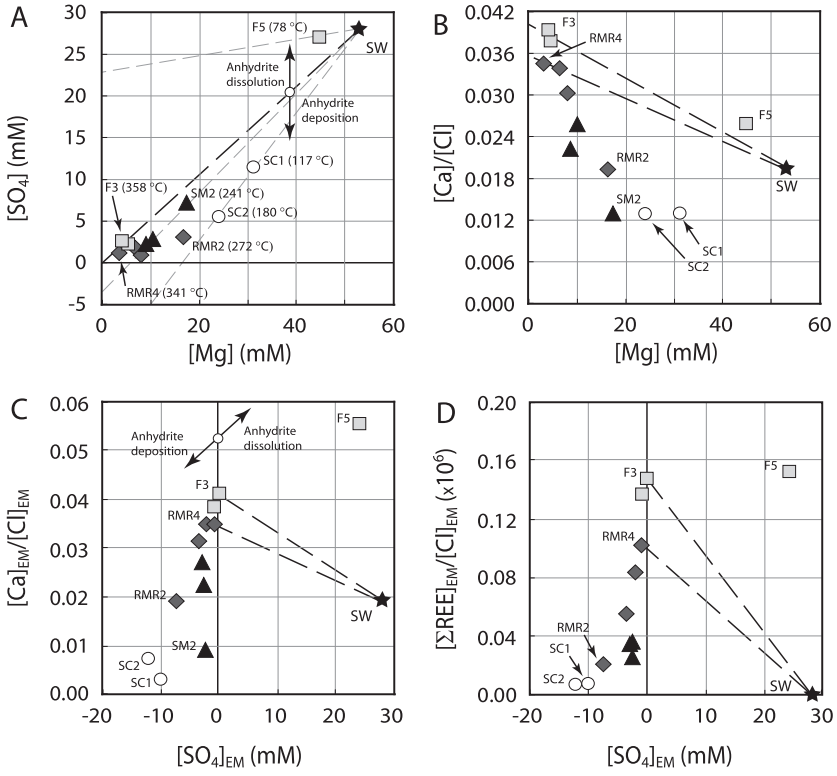

Fig. 10. Compositions of black/gray-smoker fluids from PACMANUS. (A) sulfate versus Mg; (B) chloride-normalized Ca versus Mg; (C) chloride-normalized end-member Ca versus end-member sulfate; and (D) chloride-normalized end-member REE versus end-member sulfate. Symbols as follows: Roman Ruins, gray diamonds; Satanic Mills, black triangles; Fenway, light-gray squares; Snowcap, open circles. The composition of ambient seawater is shown by the star. Normalization of calcium to chloride removes differences in Ca concentrations among hydrothermal fluids from individual vent areas resulting from sub-seafloor phase separation. Conservative mixing lines between end-member (zero Mg, zero sulfate) hydrothermal fluid ($\gg$300 °C) and seawater are shown by the black dashed lines in each plot. Many lower temperature (<280 °C) vent fluids have measurable Mg and sulfate owing to local entrainment and sub-seafloor mixing of seawater with end-member hydrothermal fluid (A). Measured sulfate, Ca and REE concentrations in many lower temperature fluids are, however, less than that predicted by conservative mixing owing to removal during anhydrite (CaSO4) precipitation (fluids SC1, SC2, RMR2, SM2). The extent of anhydrite precipitation is indicated by the magnitude of the negative sulfate end-member anomaly. In contrast, low-temperature fluids from Fenway (fluid F5) show excess sulfate, Ca and REE concentrations relative to those predicted by conservative mixing, suggesting current dissolution of previously deposited anhydrite in the Fenway mound.

fluids sampled at PACMANUS have near zero Mg and sulfate concentrations, whereas lower temperature (<280 °C) smoker fluids exhibit a range of higher Mg and sulfate concentrations consistent with mixing between end-member high-temperature hydrothermal fluids and locally entrained Mg- and sulfate-rich seawater (Reeves, 2010)(Table 1; Fig. 10). Measured sulfate concentrations in most lower temperature fluids are, however, significantly less than that predicted by conservative mixing between end-member hydrothermal fluid (zero Mg and SO_4) and ambient seawater causing measured sulfate concentrations to extrapolate to negative values at zero Mg. Although the value has no true physical meaning, the magnitude of the negative end-member concentration represents a proxy for the extent of non-conservative sulfate removal during fluid mixing. Lower temperature fluids also exhibit Ca concentrations less than that predicted by conservative mixing between end-member hydrothermal fluid and ambient seawater (Fig. 10B). The extent of non-conservative Ca removal is correlated with that of sulfate (Fig. 10C) and is explained by anhydrite precipitation during near-seafloor mixing of high-temperature hydrothermal fluids and locally entrained seawater. The REEs exhibit non-conservative behavior similar to Ca during fluid mixing suggesting that anhydrite precipitation has caused measurable removal of aqueous REEs (Fig. 10D). On the basis of the observed correlations and the magnitude of the negative sulfate end-member concentrations, on-going deposition of anhydrite appears most prevalent at the Snowcap and Roman Ruins (PACMANUS) vent areas.

Measured Mg concentrations in low-temperature (~78 °C) fluids exiting diffusely from the seafloor at Fenway (fluid F5) are near seawater concentration and are consistent with large-scale entrainment of seawater by ascending high-temperature hydrothermal fluids within the Fenway mound (Table 1). Sulfate and Ca concentrations in these diffuse fluids are higher than that predicted by conservative mixing between parent high-temperature hydrothermal fluids and seawater (Fig 10A and B), suggesting that local dissolution of previously deposited anhydrite is on-going in some fluids at Fenway in response to low fluid temperatures that enhance anhydrite solubility (Bischoff and Seyfried, 1978). Dissolution of anhydrite yields end-member sulfate and Ca concentrations in diffuse fluids that are higher than in the highest-temperature black smoker fluids at zero Mg (Fig. 10C). End-member REE concentrations in diffuse fluids at Fenway are also higher than in parent high-temperature vent fluids (Fig. 10D) and are interpreted as reflecting addition of REEs to solution as a result of anhydrite dissolution. It should be recognized that high end-member concentrations of sulfate, Ca and REEs in diffuse fluids are an artifact of extrapolation to zero Mg and should not be interpreted as indicating the actual existence of a high-temperature fluid with the specified zero Mg composition. Anhydrite dissolution represents a potential significant source of REEs because total REE concentrations in massive anhydrites recovered at the seafloor at Fenway reach values as high as 50 ppm and are enriched by several orders of magnitude relative to total REE concentrations in high-temperature hydrothermal fluids (Craddock and Bach, 2010). The REE_N patterns of high- and low-temperature hydrothermal fluids and of massive anhydrites at Fenway are similar (Craddock and Bach, 2010) indicating that dissolution of anhydrite does not, however, affect relative REE_N distributions among the sampled Fenway vent fluids.

6. SUMMARY AND CONCLUSIONS

Rare earth element data are reported for a wide range of seafloor vent fluids sampled from four hydrothermal systems in the Manus back-arc basin (Vienna Woods, PACMANUS, DESMOS and SuSu Knolls). Chondrite-normalized REE_N distribution patterns of Manus vent fluids show a wide range of compositions, which contrast with the uniform REE_N distribution patterns of mid-ocean ridge (MOR) hydrothermal fluids. These differences are correlated with differences in fluid composition, in particular pH and ligand (chloride, fluoride and sulfate) abundances. Vent fluid REE_N distribution patterns are not obviously correlated to differences in crustal rock REE compositions. The results imply that REE compositions of hydrothermal fluids are controlled predominantly by conditions of fluid–rock interaction (i.e., pH, temperature, availability of complexing ligands), which affect the relative solubility and mobilization of the REEs. Our data are supported by experimental studies that have documented fractionation of the REEs during high-temperature fluid–rock reaction (e.g., Bach and Irber, 1998; Allen and Seyfried, 2005).

In the Manus Basin, the range of REE_N patterns observed in seafloor vent fluids is interpreted as reflecting heterogeneous solubility/mobility of the REEs during fluid–rock interaction owing to the formation of REE-chloride, REE-fluoride and REE-sulfate complexes with a range of aqueous stabilities. The range of fluoride and sulfate concentrations measured in Manus hydrothermal fluids is attributed to differing amounts and styles of magmatic acid volatile (i.e., H_2O–CO_2–HCl–HF–SO_2) degassing (Gamo et al., 1997; Douville et al., 1999; Seewald et al., 2006; Reeves, 2010). A significant implication of our results are that REE distributions in seafloor hydrothermal fluids can be used as indicators of styles of magmatic degassing at depth. It has been proposed that the uniform REE_N pattern of MOR hydrothermal fluids (i.e., light-REE enrichment and positive Eu anomaly) primarily reflects exchange of REE during plagioclase recrystallization (Campbell et al., 1988; Klinkhammer et al., 1994; Douville et al., 1999). The results of this study, however, suggest that a light-REE enrichment and positive Eu anomaly reflect enhanced mobility of the light-REEs and Eu owing to the predominance of REE-chloride complexes in chloride-rich and fluoride- and sulfate-poor MOR hydrothermal fluids. Local processes, including sub-surface fluid mixing and mineral deposition and remobilization, may also affect REE concentrations of seafloor hydrothermal fluids. However, REE_N distributions of seafloor vent fluids are primarily affected by key aspects of fluid composition (e.g., pH, ligand concentration) that affect REE speciation and mobility during fluid–rock interaction at depth.

This detailed study of REE compositions of seafloor vent fluids indicates that REEs can provide critical information about fundamental sub-seafloor geochemical processes associated with hydrothermal activity, including conditions of fluid–rock interaction and the extent and styles of magmatic acid volatile degassing. A better understanding of aqueous REE behavior offers important constraints for interpreting REE signatures preserved in the mineral record. Future studies of REE-bearing mineral deposits can be used to gain insight about geochemical processes pertaining to hydrothermal vent deposit formation and are essential for inactive and relict systems where access to hydrothermal fluids is precluded.

ACKNOWLEDGMENTS

The authors acknowledge the Captain and crew of the *R/V Melville* and the *ROV Jason II* technical group for a very successful cruise and sample collection. P. Saccocia and E. Walsh provided great help during shipboard fluid sample processing. D. Schneider and S. Birdwhistell (WHOI) are acknowledged for assistance during rare earth element analysis by ICP–MS. Reviews by A.A. Migdisov and an anonymous reviewer provided critical, constructive and thought-provoking comments that greatly aided in the discussion and presentation of our research. The authors thank the Associate Editor, J.-I. Ishibashi, for his editorial assistance and supportive and insightful comments. This study received financial support from the Ocean Drilling Program Schlanger Fellowship (to P.R. Craddock), the WHOI Deep Ocean Exploration Institute Graduate Fellowship (to E. Reeves) and NSF Grant OCE-0327448.

APPENDIX A. SUPPLEMENTARY DATA

Supplementary data associated with this article can be found, in the online version, at doi:10.1016/j.gca.2010.07.003.

REFERENCES

Allen D. E. and Seyfried, Jr., W. E. (2005) REE controls in ultramafic hosted MOR hydrothermal systems: an experimental study at elevated temperature and pressure. *Geochim. Cosmochim. Acta* **69**(3), 675–683.

Bach W. and Irber W. (1998) Rare earth element mobility in the oceanic lower sheeted dyke complex: evidence from geochemical data and leaching experiments. *Chem. Geol.* **151**(1), 309–326.

Bach W., Roberts S., Vanko D. A., Binns R. A., Yeats C. J., Craddock P. R. and Humphris S. E. (2003) Controls of fluid chemistry and complexation on rare-earth element contents of anhydrite from the Pacmanus subseafloor hydrothermal system, Manus Basin, Papua New Guinea. *Miner. Deposita* **38**(8), 916–935.

Bach W., Tivey M. A., Seewald J. S., Tivey M. K., Craddock P. R., Niedermeier D. and Yoerger D. (2007) Variable basement composition and magma degassing affecting hydrothermal systems in the Eastern Manus Basin. *EOS Trans. AGU. Fall Meet. Suppl.* **88**(52). Abstract #V21D-0749.

Bau M. (1991) Rare-earth element mobility during hydrothermal and metamorphic fluid–rock interaction and the significance of the oxidation state of europium. *Chem. Geol.* **93**(3–4), 219–230.

Bau M. and Dulski P. (1999) Comparing yttrium and rare earths in hydrothermal fluids from the Mid-Atlantic Ridge: implications for Y and REE behaviour during near-vent mixing and for the Y/Ho ratio of Proterozoic seawater. *Chem. Geol.* **155**(1), 77–90.

Beaudoin Y., Scott S. D., Gorton M. P., Zajacz Z. and Halter W. (2007) Effects of hydrothermal alteration on Pb in the active PACMANUS hydrothermal field, ODP Leg 193, Manus Basin, Papua New Guinea: a LA-ICP-MS study. *Geochim. Cosmochim. Acta* **71**(17), 4256–4278.

Bethke C. M. (1996) *Geochemical Reaction Modeling*. Oxford University Press.

Binns R. A., Barriga F. J. A. S. and Miller, D. J. (2007) Leg 193 synthesis: anatomy of an active felsic-hosted hydrothermal system, eastern Manus Basin, Papua New Guinea. In *Proceedings of the Ocean Drilling Program, Scientific Results* (eds. F. J. A. S. Barriga, R. A. Binns, D. J. Miller and P. M. Herzig), **vol. 193**. pp. 1–71. doi:10.2973/odp.proc.sr.193.201.2007 (Ocean Drilling Program).

Binns R. A. and Scott S. D. (1993) Actively forming polymetallic sulfide deposits associated with felsic volcanic rocks in the eastern Manus back-arc basin, Papua New Guinea. *Econ. Geol.* **88**, 2226–2236.

Binns R. A., Scott S. D., Gemmell J. B., Crook K. A. W., and Shipboard Scientific Party (1997) The SuSu Knolls hydrothermal field, eastern Manus Basin, Papua New Guinea. *EOS Trans. AGU. Fall Meet. Suppl.* **78**(52) (abstr. #V22E-02).

Bischoff J. L. and Seyfried, Jr., W. E. (1978) Hydrothermal chemistry of seawater from 25 to 350 °C. *Am. J. Sci.* **278**, 838–860.

Both R., Crook K., Taylor B., Brogan S., Chappell B., Frankel E., Liu L., Sinton J. and Tiffin D. (1986) Hydrothermal chimneys and associated fauna in the Manus back-arc basin, Papua New Guinea. *EOS Trans. Am. Geophys. Union* **67**, 489.

Campbell A. C., Palmer M. R., Klinkhammer G. P., Bowers T. S., Edmond J. M., Lawrence J. R., Casey J. F., Thompson G., Humphris S. E. and Rona P. (1988) Chemistry of hot springs on the Mid-Atlantic Ridge. *Nature* **335**(6190), 514–519.

Craddock, P. R. 2009. *Geochemical Tracers of Processes Affecting the Formation of Seafloor Hydrothermal Fluids and Deposits in the Manus Back-arc Basin*. Ph. D. thesis, Massachusetts Institute of Technology-Woods Hole Oceanographic Institution, Woods Hole, MA, 370pp.

Craddock P. R. and Bach W. (2010) Insights to magmatic-hydrothermal processes in the Manus back-arc basin as recorded by anhydrite. *Geochim. Cosmochim. Acta* **74**(19), 5514–5536.

Davies H. L., Honza E., Tiffin D. L., Lock J., Okuda Y., Keene J. B., Murakami F. and Kisimoto K. (1987) Regional setting and structure of the western Solomon Sea. *Geo-Marine Lett.* **7**, 153–160.

Douville E., Bienvenu P., Charlou J. L., Donval J. P., Fouquet Y., Appriou P. and Gamo T. (1999) Yttrium and rare earth elements in fluids from various deep-sea hydrothermal systems. *Geochim. Cosmochim. Acta* **63**(5), 627–643.

Edmond J. M., Campbell A. C., Palmer M. R., German C. R., Klinkhammer G. P., Edmonds H. N., Elderfield H., Thompson G., and Rona P. (1995) Time series studies of vent fluids from the TAG and MARK sites (1986, 1990) Mid-Atlantic Ridge and a mechanism for Cu/Zn zonation in massive sulphide orebodies. In *Hydrothermal Vents and Processes* (eds. L. M. Parson, C. L. Walker, and D. R. Dixon), **vol. 87**. Geological Society Special Publication. pp. 77–86.

Fulignati P., Gioncada A. and Sbrana A. (1999) Rare-earth element (REE) behaviour in the alteration facies of the active magmatic-hydrothermal system of Vulcano (Aeolian Islands, Italy). *J. Volcanol. Geotherm. Res.* **88**(4), 325–342.

Gammons C. H., Wood S. A., and Youning L. (2002). Complexation of the rare earth elements with aqueous chloride at 200 °C and 300 °C and saturated water vapor pressure. In *Water–Rock Interaction, Ore Deposits and Environmental Geochemistry: A Tribute to David A. Crerar*. (eds. R. Hellmann and S. A. Wood), **vol. 7**. The Geochemical Society Special Publication. pp. 191–207.

Gamo T., Okamura K., Charlou J. L., Urabe T., Auzende J. M., Ishibashi J.-I., Shitashima K., Chiba H., Binns R. A. and Gena K. (1997) Acidic and sulfate-rich hydrothermal fluids from the Manus back-arc basin, Papua New Guinea. *Geology* **25**(2), 139–142.

Gena K., Mizuta T., Ishiyama D. and Urabe T. (2001) Acid-sulphate type alteration and mineralization in the Desmos Caldera, Manus back-arc basin, Papua New Guinea. *Resour. Geol.* **51**(1), 31–44.

Giggenbach W. F. (1992) Isotopic shifts in waters from geothermal and volcanic systems along convergent plate boundaries and their origin. *Earth Planet. Sci. Lett.* **113**, 495–510.

Gimeno Serrano M. J., Auque Sanz L. F. and Nordstrom D. K. (2000) REE speciation in low-temperature acidic waters and the competitive effects of aluminum. *Chem. Geol.* **165**(3–4), 167–180.

Haas J. R., Shock E. L. and Sassani D. C. (1995) Rare earth elements in hydrothermal systems: estimates of standard partial molal thermodynamic properties of aqueous complexes of the rare earth elements at high pressures and temperatures. *Geochim. Cosmochim. Acta* **59**(21), 4329–4350.

Hanson G. N. (1980) Rare earth elements in petrogenetic studies of igneous systems. *Annu. Rev. Earth Planet. Sci.* **8**(1), 371–406.

Hedenquist J. W., Aoki M. and Shinohara H. (1994) Flux of volatiles and ore-forming metals from the magmatic-hydrothermal system of Satsuma Iwojima Volcano. *Geology* **22**(7), 585–588.

Hemley J. J., Hostetler P. B., Gude A. J. and Mountjoy W. T. (1969) Some stability relations of alunite. *Econ. Geol.* **64**, 599–612.

Hemley J. J. and Jones W. R. (1964) Chemical aspects of hydrothermal alteration with emphasis on hydrogen metasomatism. *Econ. Geol.* **59**, 538–569.

Holland H. D. (1965) Some applications of thermochemical data to problems of ore deposits; [**II**] Mineral assemblages and the composition of ore forming fluids. *Econ. Geol.* **60**(6), 1101–1166.

Hrischeva E., Scott S. D. and Weston R. (2007) Metalliferous sediments associated with presently forming volcanogenic massive sulfides: The SuSu Knolls hydrothermal field, Eastern Manus Basin, Papua New Guinea. *Econ. Geol.* **102**, 55–74.

Humphris S. E. (1998) Rare earth element composition of anhydrite: Implications for deposition and mobility within the TAG hydrothermal mound. In *Proceedings of the Ocean Drilling Program, Scientific Results* (ed. P. M. Herzig, S. E. Humphris, D. J. Miller, and R. A. Zierenberg), **vol. 158**. Ocean Drilling Program. pp. 143–159.

Humphris S. E. and Bach W. (2005) On the Sr isotope and REE compositions of anhydrites from the TAG seafloor hydrothermal system. *Geochim. Cosmochim. Acta* **69**, 1511–1525.

Johnson J. W., Oelkers E. H. and Helgeson H. C. (1992) SUPCRT 92: a software package for calculating the standard molal thermodynamic properties of minerals, gases, aqueous species and reactions from 1 to 5000 bar, and 0 to 1000 °C. *Comput. Geosci.* **18**(7), 899–947.

Klinkhammer G. P., Elderfield H., Edmond J. M. and Mitra A. (1994) Geochemical implications of rare earth element patterns in hydrothermal fluids from mid-ocean ridges. *Geochim. Cosmochim. Acta* **58**(23), 5105–5113.

Lackschewitz K. S., Devey C. W., Stoffers P., Botz R., Eisenhauer A., Kummetz M., Schmidt M. and Singer A. (2004) Mineralogical, geochemical and isotopic characteristics of hydrothermal alteration processes in the active, submarine, felsic-hosted PACMANUS field, Manus Basin, Papua New Guinea. *Geochim. Cosmochim. Acta* **68**(21), 4405–4427.

Lewis A. J., Komninou A., Yardley B. W. D. and Palmer M. R. (1998) Rare earth element speciation in geothermal fluids from Yellowstone National Park, Wyoming, USA. *Geochim. Cosmochim. Acta* **62**(4), 657–663.

Lewis A. J., Palmer M. R., Sturchio N. C. and Kemp A. J. (1997) The rare earth element geochemistry of acid-sulphate and acid-sulphate-chloride geothermal systems from Yellowstone National Park, Wyoming, USA. *Geochim. Cosmochim. Acta* **61**(4), 695–706.

Martinez F. and Taylor B. (1996) Backarc spreading, rifting, and microplate rotation, between transform faults in the Manus Basin. *Marine Geophys. Res.* **18**, 203–224.

Michard A. (1989) Rare earth element systematics in hydrothermal fluids. *Geochim. Cosmochim. Acta* **53**, 745–750.

Michard A. and Albarede F. (1986) The REE content of some hydrothermal fluids. *Chem. Geol.* **55**(1–2), 51–60.

Michard G., Albarède F., Michard A., Minster J. F. and Charlou J. L. (1983) Rare-earth elements and uranium in high-temperature solutions from East Pacific Rise hydrothermal vent field (13 °N). *Nature* **303**, 795–797.

Migdisov A. A. and Williams-Jones A. E. (2007) An experimental study of the solubility and speciation of NdF_3 in F-bearing aqueous solutions. *Geochim. Cosmochim. Acta* **71**, 3056–3069.

Migdisov A. A., Williams-Jones A. E. and Wagner T. (2009) An experimental study of the solubility and speciation of the rare earth elements (**III**) in fluoride- and chloride-bearing aqueous solutions at temperatures up to 300 °C. *Geochim. Cosmochim. Acta* **73**, 7087–7109.

Miller D. J., Vanko D. A., and Paulick H. (2006). Data report: petrology and geochemistry of fresh, recent dacite lavas at Pual Ridge, Papua New Guinea, from an active, felsic-hosted seafloor hydrothermal system. In *Proceedings of the Ocean Drilling Program, Scientific Results* (eds. F. J. A. S. Barriga, R. A. Binns, D. J. Miller, and P. M. Herzig), vol. 193. Ocean Drilling Program. pp. 1–31. doi:10.2973/odp.proc.sr.193.208.2006.

Mills R. A. and Elderfield H. (1995) Rare earth element geochemistry of hydrothermal deposits from the active TAG Mound, 26 °N Mid-Atlantic Ridge. *Geochim. Cosmochim. Acta* **59**, 3511–3524.

Mills R. A., Teagle D. A. H. and Tivey, M. K. (1998) Fluid mixing and anhydrite precipitation within the TAG mound. In *Proceedings of the Ocean Drilling Program, Scientific Results* (eds. P. M. Herzig, S. E. Humphris, D. J. Miller, and R. A. Zierenberg), vol. 158. Ocean Drilling Program. pp. 119–127.

Mills R. A. and Tivey M. K. (1999) Sea water entrainment and fluid evolution within the TAG hydrothermal mound: Evidence from analyses of anhydrite. In *Mid-Ocean Ridges: Dynamics of Processes Associated with Creation of New Ocean Crust* (eds. J. R. Cann, H. Elderfield and A. Laughton). Cambridge University Press, pp. 225–248.

Mitra A., Elderfield H. and Greaves M. J. (1994) Rare earth elements in submarine hydrothermal fluids and plumes from the Mid-Atlantic Ridge. *Marine Chem.* **46**(3), 217–235.

Möller P. (2002) The distribution of rare earth elements and yttrium in water–rock interactions: field observations and experiments. In *Water–Rock Interaction* (eds. I. Stober and K. Bucher). Kluwer Academic Publishers, pp. 97–123.

Paulick H. and Bach W. (2006) Phyllosilicate alteration mineral assemblages in the Active Subsea-Floor Pacmanus Hydrothermal System, Papua New Guinea, ODP Leg 193. *Econ. Geol.* **101**, 633–650.

Paulick H., Herzig P. M., and Hoernes, S. (2005) Data report: a comprehensive geochemical, mineralogical and isotopic dataset of altered dacitic volcanic rocks from the subsurface of the PACMANUS hydrothemal field (ODP Leg 193). In *Proceedings of the Ocean Drilling Program, Scientific Results* (eds. F. J. A. S. Barriga, R. A. Binns, D. J. Miller, and P. M. Herzig), vol. 193. Ocean Drilling Program. pp. 1–18. doi:10.2973/odp.proc.sr.193.209.2005.

Reeves E. (2010) Laboratory and field-based investigations of subsurface geochemical processes in seafloor hydrothermal systems. Ph. D. thesis, Massachusetts Institute of Technology-Woods Hole Oceanographic Institution, Woods Hole, MA.

Roberts S., Bach W., Binns R. A., Vanko D. A., Yeats C. J., Teagle D. A. H., Blacklock K., Blusztajn J. S., Boyce A. J. and Cooper M. J. (2003) Contrasting evolution of hydrothermal fluids in the PACMANUS system, Manus Basin: The Sr and S isotope evidence. *Geology* **31**(9), 805–808.

Sakai H., Gamo T. and Scientific, Crew of Cruise KH-90-3 (1991). Hydrothermal activity in the eastern Manus Basin, Bismarck Sea: A brief report of the Hakuho-Maru Cruise KH-90-3. *Ridge Events* **2**, 39–51.

Schnetzler C. C. and Philpotts J. A. (1970) Partition coefficients of rare-earth elements between igneous matrix material and rock-forming mineral phenocrysts-II. *Geochim. Cosmochim. Acta* **34**, 331–340.

Seewald J. S., Doherty K. W., Hammar T. R. and Liberatore S. P. (2002) A new gas-tight isobaric sampler for hydrothermal fluids. *Deep Sea Res. Part I: Oceanograph. Res. Pap.* **49**(1), 189–196.

Seewald J. S., Reeves E., Saccocia P., Rouxel O. J., Walsh E., Price R. E., Tivey M., Bach W., and Tivey M. (2006). Water–rock reaction, substrate composition, magmatic degassing, and mixing as major factors controlling vent fluid compositions in Manus Basin hydrothermal systems. *EOS Trans. AGU. Fall Meet. Suppl.* **87**(52) Abstract #B34A-02.

Sinton J. M., Ford L. L., Chappell B. and McCulloch M. T. (2003) Magma genesis and mantle heterogeneity in the Manus Back-Arc Basin, Papua New Guinea. *J. Petrol.* **44**, 159–195.

Sun W. D., Binns R. A., Fan A. C., Kamenetsky V. S., Wysoczanski R., Wei G. J., Hu Y. H. and Arculus R. J. (2007) Chlorine in submarine volcanic glasses from the eastern Manus basin. *Geochim. Cosmochim. Acta* **71**, 1542–1552.

Sverjensky D. A. (1984) Europium redox equilibria in aqueous solution. *Earth Planet. Sci. Lett.* **67**, 70–78.

Taylor B. (1979) Bismarck Sea; evolution of a back-arc basin. *Geology* **7**, 171–174.

Tivey M. A., Bach W., Seewald J. S., Tivey M. K., Vanko D. A., and Shipboard Science and Technical Teams (2007) Cruise report R/V Melville, MAGELLAN-06. In *Hydrothermal Systems in the Eastern Manus Basin: Fluid Chemistry and Magnetic Structures as Guides to Subseafloor Processes*. Woods Hole Oceanographic Institution. p. 67.

Tivey M. K., Humphris S. E., Thompson G., Hannington M. D. and Rona P. A. (1995) Deducing patterns of fluid flow and mixing within the TAG active hydrothermal mound using mineralogical and geochemical data. *J. Geophys. Res.* **100**(B7), 12527–12555.

Tivey M. K., Mills R. A., and Teagle D. A. H. (1998). Temperature and salinity of fluid inclusions in anhydrite as indicators of seawater entrainment and heating within the TAG active mound. In *Proceedings of the Ocean Drilling Program, Scientific Results* (eds. P. M. Herzig, S. E. Humphris, D. J. Miller, and R. A. Zierenberg), **vol. 158**. Ocean Drilling Program. pp. 179–190.

Tufar W. (1990) Modern hydrothermal activity, formation of complex massive sulfide deposits and associated vent communities in the Manus back-arc basin (Bismarck Sea, Papua New Guinea). *Mitt. Österr. Geol. Ges.* **82**, 183–210.

Von Damm K. L. (1983) Chemistry of submarine hydrothermal solutions at 21° North, East Pacific Rise and Guaymas Basin, Gulf of California. Ph. D. thesis, Massachusetts Institute of Technology-Woods Hole Oceanographic Institution.

Von Damm K. L., Edmond J. M., Grant B., Measures C. I., Walden B. and Weiss R. F. (1985) Chemistry of submarine hydrothermal solutions at 21 °N, East Pacific Rise. *Geochim. Cosmochim. Acta* **49**(11), 2197–2220.

Wood S. A. (1990) The aqueous geochemistry of the rare-earth elements and yttrium: 2. Theoretical predictions of speciation in hydrothermal solutions to 350 °C at saturation water vapor pressure. *Chem. Geol.* **88**(1–2), 99–125.

Wood S. A. (2001) Behavior of rare earth elements in geothermal systems: a new exploration/exploitation tool? US Department of Energy Report, University of Idaho, Moscow, ID, p. 35.

Yeats C. J., Binns R. A. and Parr J. M. (2000) Advanced argillic alteration associated with actively forming submarine polymetallic sulfide mineralization in the eastern Manus Basin, Papua New Guinea. *Geol. Soc. Aust. Abstr.* **59**, 555.

Associate Editor: Jun-Ichiro Ishibashi